University Mohamed Khider de Biskra
Faculty of Exact Sciences and Sciences of Nature and Life
Matter Sciences Department

Dissertation of Master

Filed of Matter Sciences
Physics
Physics of Materials

Ref. :

Presented by :
Chenaf Kaouther
The :

Study of graphene-based solar cells by simulation

Jury :

Tibermacine Toufik	M.C.A	Mehamed Khider University -Biskra	President
Boumaraf Rami	M.C.B	Mehamed Khider University -Biskra	Supervisor
Laznek Samira	M.C.B	Mehamed Khider University -Biskra	Examiner

Academic year : 2020/2021

# ACKNOWLEDGEMENT

*First and foremost, praises and thanks to **"ALLAH"**, the Almighty, for His showers of blessings throughout my research work to complete the research successfully.*

*I would like to express my deep and sincere gratitude to my research supervisor **Dr.Boumaraf Rami**.*

*I am extremely grateful to my parents **"Chenaf Bachir"** and **"Souiki Leila"** for their love, prayers, caring and sacrifices for educating and preparing me for my future.*

*I also thank my brothers**(Ilyes, Abdelrachid, Abdelwahab, Chakir** and **Zoubir),** my only sister **(Zaineb),** Our family's children(**Younes, Anes, Adam** and **Tamim**) and my friends **(Imen Bou, Ikram, Siham, Nour, Imen Ch, Amira, Marwa, Souhila, Yassmine, Ahlem, Nadjah,Maha, Sara, Fairouze, Soumia, Kaouther, Bouthaina, Chaima…)***

*I would not forget to thank the members of the jury, **Dr. Toufik Tibermacine** and **Dr. Laznek Samira** who have kindly accepted to read and examine our work.*

Finally, my thanks go to all the people who have supported me to complete the research work directly or indirectly.

KAOUTHER

Abstrat

Since the discovery of graphene in 2004, researchers have carried out several researches to study its distinctive properties of high transparency, great conductivity, and superior flexibility, and its impact on the field of contemporary electronics, especially in the field of solar energy.

In this thesis, we have performed a simulation of a graphene-based solar cell using the SILVACO TCAD semiconductor device simulation program, which was used to simulate the effect of various physical parameters such as thickness and work function on the electrical properties of the solar cell, Jsc (short-circuit current density), Voc (circuit voltage Open), FF (Fill Factor), Eff (energy conversion efficiency) , where this simulation was performed under AM1.5 irradiation.

Key words: Simulation, Silvaco atlas, Graphene, solar cell.

Résumé

Depuis la découverte du graphène en 2004, les chercheurs ont mené plusieurs recherches pour étudier ses propriétés distinctives de haute transparence, de grande conductivité et de flexibilité supérieure, ainsi que son impact sur le domaine de l'électronique contemporaine, en particulier dans le domaine de l'énergie solaire.

Dans cette thèse, nous avons effectué une simulation d'une cellule solaire à base de graphène à l'aide du programme de simulation de dispositif semi-conducteur SILVACO TCAD, qui a été utilisé pour simuler l'effet de divers paramètres physiques tels que l'épaisseur et la fonction de travail sur les propriétés électriques de la cellule solaire. , Jsc (densité de courant de court-circuit), Voc (tension de circuit ouvert) , FF , Eff (efficacité de conversion d'énergie) , où cette simulation a été réalisée sous irradiation AM1.5.

Les mots clés : Simulation, Atlas de Silvaco, Graphène, les cellules solaires.

ملخص

منذ اكتشاف الجرافين في عام 2004 أجرى الباحثون العديد من الأبحاث لدراسة خصائصه المميزة للشفافية العالية والموصلية العالية والمرونة الفائقة ، وتأثيره على مجال الإلكترونيات المعاصرة وخاصة في مجال الطاقة الشمسية.

في هذه الأطروحة ، أجرينا محاكاة لخلية شمسية القائمة على الجرافين باستخدام برنامج محاكاة جهاز أشباه الموصلات SILVACO TCAD ، والذي تم استخدامه لمحاكاة تأثير مختلف المعلمات الفيزيائية مثل السماكة ووظيفة العمل على الخواص الكهربائية للخلية الشمسية ، Jsc(كثافة تيار الدائرة القصيرة) ، Voc (جهد الدائرة المفتوحة) ،FF (معامل التعبئة) ، Eff(كفاءة تحويل الطاقة) ، حيث تم إجراء هذه المحاكاة تحت إشعاع AM1.5.

الكلمات المفتاحية: محاكاة، سيلفاكو أطلس، الجرافين، الخلايا الشمسية .

Table of contents

Chaptre 3 : SILVACO simulation and results

LIST OF FIGURE

LIST OF TABLE

LIST OF SYMBOLS

SBH	The Schottky barrier height
AM 1.5	Standard terrestrial solar spectrums ‘Air Mass 1.5’
Si	Silicone
PCE	Power conversion efficiency
FF	Fill factor
Voc	Open circuit voltage
Jsc	Short circuit current
J-V	Current-density vs. voltage
$\boldsymbol{\lambda}$	Wavelength
$\boldsymbol{h}$	Planck's constant
$\boldsymbol{c}$	The speed of light in a vacuum
$\boldsymbol{Eg}$	The gap energy
$\mathbf{I}_{ph}$	Photo-generated current by the solar generator under illumination
$\mathbf{I}_{s}$	Saturation current of the solar cell
K_B	Boltzmann constant
η	Ideal factor of the solar cell
T	Temperature
Q	Electric charge
E	Intensity of illumination in W/Cm^2
S	The area of the solar cell

Φ_m	Work function of the metal
Φ_B	The potential barrier of Schottky
χ	Affinity
V_{BI}	The built-in potential
φ	The electrostatic potential
ε_0	The permittivity of free space
ε	The static relative permittivity of the medium
n	Electron
p	Hole
D_n .	Diffusion constant of the electrons
Dp	Diffusion constant of the holes.
μ_n	Electron mobility
μ_p	Hole mobility
FLG	Few-Layer Graphene
MLG	Multi-Layer Graphene
GO	Graphene Oxide
rGO	Reduced Graphene Oxide
CVD	Chemical vapor deposition
CdTe	Cadmium Telluride
CIGS	Copper-Indium-Gallium-Selenide
FhG-ISE	Fraunhofer Institut für Solare Energiesysteme
AIST	Japanese National Institute of Advanced Industrial Science and Technology

NREL	National Renewable Energy Laboratory.

Introduction

Introduction

The sudden increase in global energy demand is prompting the scientific community to find alternative, cheap and efficient solutions to exploit renewable sources. In this context, current photovoltaic technologies, such as silicon-based, organic and perovskite solar cells are gaining an increasingly important role.

The main challenge is to harvest solar energy in an efficient manner by exploiting a technology that is cost effective, scalable and durable. In this context, two-dimensional (2D) materials have attracted great interest due to their exciting optical and electronic properties. Moreover, due to its atomic-thin dimensions and high versatility, 2D materials can be combined with future generation of photovoltaic devices, enhancing efficiency and improving solar cell structures. In fact, graphene can be used

Graphene is a newly discovered material in 2004, containing a thin two-dimensional layer consisting of pure carbon atoms, and has exceptional advantages, its high transparency and conductivity, as an electrode in solar cells, but the dipole electrical transport makes it also suitable as a cell anode and/or cathode. Make it the focus of attention of researchers and industrialists. Despite their interest in graphene and its applications, these applications are still mostly under theoretical research, as they have not yet reached the manufacturing stage.

In this work, we will investigate the performance of graphene-based solar cells, in order to increase the conversion efficiency, by studying some effects (such as doping, thickness, work function ...etc), by simulation using the Silvaco Atlas software.

This thesis contains three chapters:

The first is an overview of solar cell principles with details.

The second chapter describes details about graphene and its use in solar cells

The third chapter is divided into two parts: the first part describes some definitions about SILVACO TCAD simulation; In the second part, it discusses and analyzes the simulation results.

Chapter 1:

Solar Cells Fundamentals

1 Introduction

Photovoltaic Solar cells are semiconductor devices that rely on the absorption of light, specifically photons, from the solar spectrum to generate electron-hole pairs. The separation and subsequent collection of these electron hole pairs is the method by which solar cells convert solar energy into useful electricity. In order to create a new solar cell design.

In this chapter, we cite some concepts about solar cells, including their (definition, solar cell structure, working principle, the current–voltage characteristics ... etc) and we will talk about the various existing generations.

2 The solar cell

2.1 Definition

Solar cell is a device that converts energy from the sun directly into electrical energy. It provides. The longest-lasting source of energy for satellites and space vehicles. It has also been successfully implemented in several small-scale terrestrial applications. Its importance has not stopped growing, especially since the world has come to realize that, it must develop other energy resources other than conventional resources. The best candidate for this function is the sun [1] .

2.2 solar cell structure

The commonly solar cell is configured as a large-area p-n junction made from silicon semi-conductor, Therefore, in order to study the photovoltaic cells we must have an understanding of the basics of the semi-conductor materials and particularly the PN junction.

2.2.1 Semiconductors

This class of materials is between metals (conductors) and insulators (non-conductors). The resistivity of semiconductors varies from 10^{-3} to 10^{4} Ω.cm. Free electrons and moving holes are the charge carriers responsible for electrical conductivity.

Semiconductors are classified according to their chemical composition. There are elementary semiconductors such as silicon (Si), germanium (Ge), and gray tin (α-Sn), all of which belong to group IV of the periodic table. There are also composite semiconductors, These elements can be of group IV, as in the case of silicon carbide, but it is more common that they are elements of other groups, the most common being semiconductors III-V , made up of elements of group III (aluminum, gallium, indium, etc.) and elements of group V (nitrogen, phosphorus, arsenic, antimony, etc.), and also there are other semi-conductor composites, binary, ternary ....., type II-VI made up of elements of group II and other elements of group VI [2] , Two main types of semiconductors are n-type and p-type semiconductors

2.2.2 The band gap

The family of semiconductor materials can be classified into two families. Direct gap materials, like most compounds from columns III-V of the periodic table and indirect gap materials like silicon (column IV). the band gap (gap energy) $\boldsymbol{Eg}$ of a semiconductor determines how a solar cell reacts to light.

The band gap of the semiconductor material determines the smallest wavelength of light needed to generate electrical energy. The relation between the band gap and the wavelength is [3] :

$$\lambda = \boldsymbol{h\ c} / Eg = 1.24 / Eg \qquad (1.1)$$

Where:

$\boldsymbol{\lambda}$: is the wavelength in μm.

$\boldsymbol{h}$: is Planck's constant.

$\boldsymbol{c}$: is the speed of light in a vacuum.

$\boldsymbol{Eg}$: is the gap energy in $\boldsymbol{eV}$ ($\boldsymbol{1eV} = \boldsymbol{1.6} \times \boldsymbol{10}\ \boldsymbol{-19J}$).

2.2.3 The PN junction

PN junctions are elementary "building blocks" of semiconductor electronic devicessuch as diodes, transistors, solar cells and integrated circuits.

• Joining n-type material with p-type material causes excess electrons in the n-type material to diffuse to the p-type side and excess holes from the p-type material to diffuse to the n-type side

• Movement of electrons to the p-type side exposes positive ion cores in the n-type side while movement of holes to the n-type side exposes negative ion cores in the p-type side, resulting in an electron field at the junction and forming the depletion region.

• A voltage results from the electric field formed at the junction [4]

as shown in figure 1:

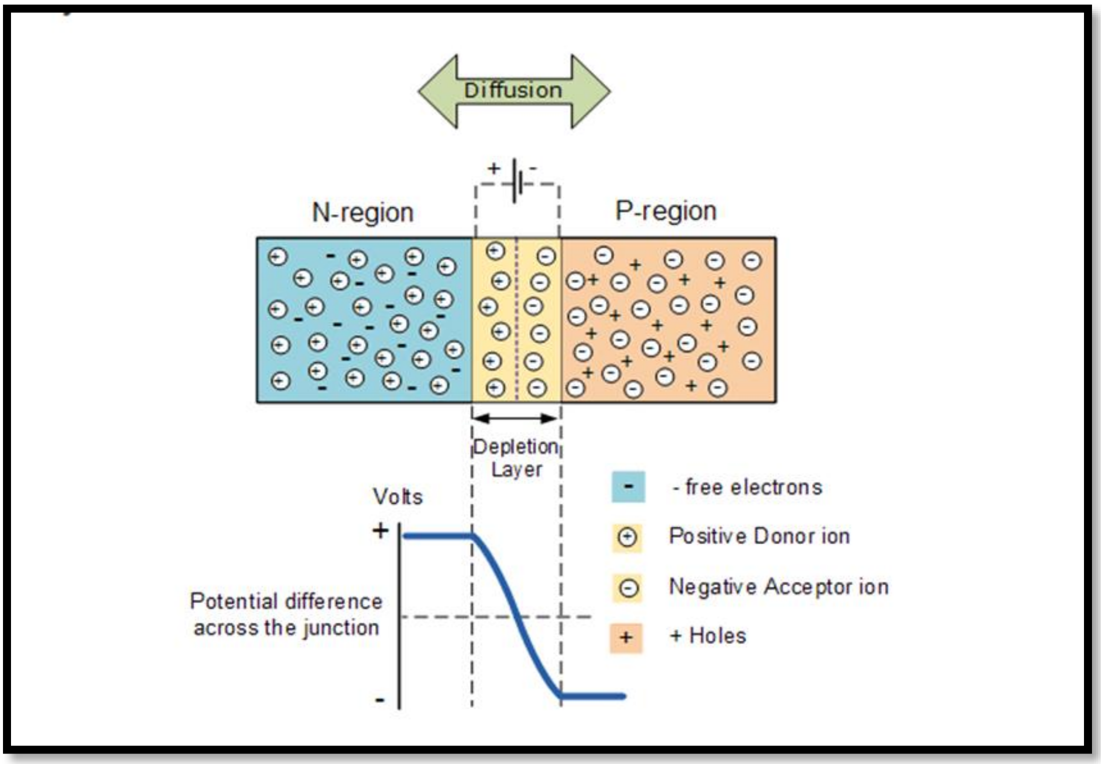

Figure1.1: The PN junction [1]

2.2.4 Schottky junction (metal/semiconductor)

Metal-semiconductor (M-S) junctions have a great importance since they are present in every semiconductor device. They can behave either as a Schottky Named after Walter Schottky barrier or as an ohmic contact dependent on the characteristics of the interface. We will primarily focus on Schottky barriers [5].

All metals have a work function Φ_m: the energy it takes to remove an electron from the atom to the vacuum level potential. The attributes of both metal and semiconductor while separated are illustrated in Figure2. The potential energy needed to inject charge carriers from the metal into the semiconductor material is the Schottky barrier height measured in electron volts (eV). The Schottky barrier height value is the energy it takes to remove an electron from the metal minus the energy required to detach an electron from the n-type semiconductor material (electron affinity) creating electron flow from the semiconductor to the metal. The Schottky barrier height may be computed for a Schottky diode by the following equation [6]:

$$\Phi_B = \Phi_m + \chi \qquad (1.2)$$

The Schottky barrier height (often referred to as SBH) is a fixed amount of energy drop across the diode, this value is unique to the combination of metal and semiconductor, ideally this does not vary with forward voltage biasing or current flow. However the phenomenon of SBH lowering may occur in reverse bias due to electric field crowding [5].

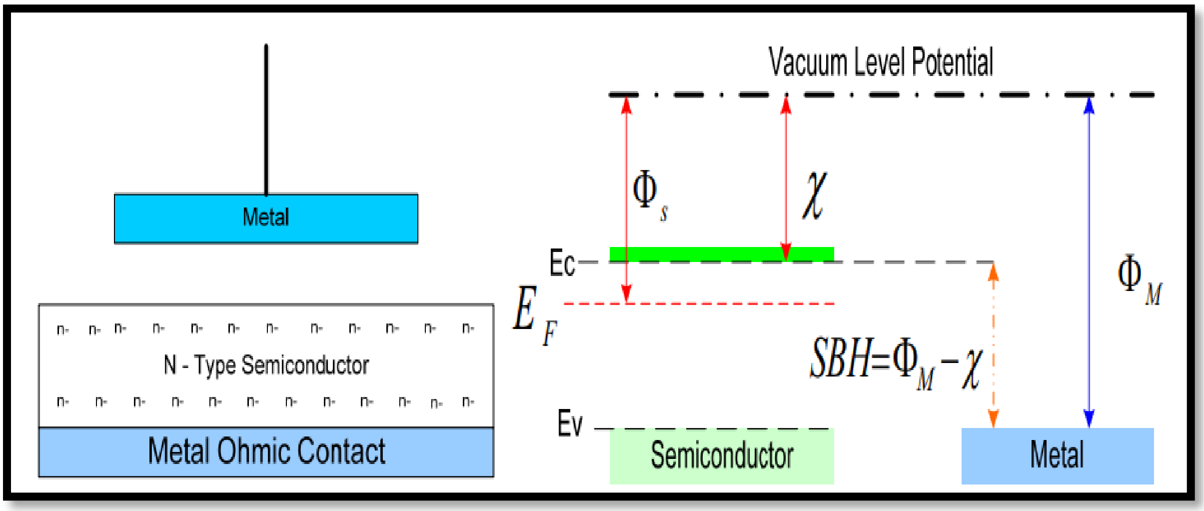

Figure1. 2: Metal and semiconductor before contact; band diagram Schottky barrier height.

When the metal contacts the semiconductor there is an imbalance of Fermi energy states in the two materials and the charges migrate to reach equilibrium levels. To simplify this matter, some of the electrons in the n-type semiconductor migrate into the metal leaving behind a region of material with no free charge carriers. This area is called the depletion region, and the energy it takes to cross this region is known as the built-in potential. This concept is illustrated in Figure 3.

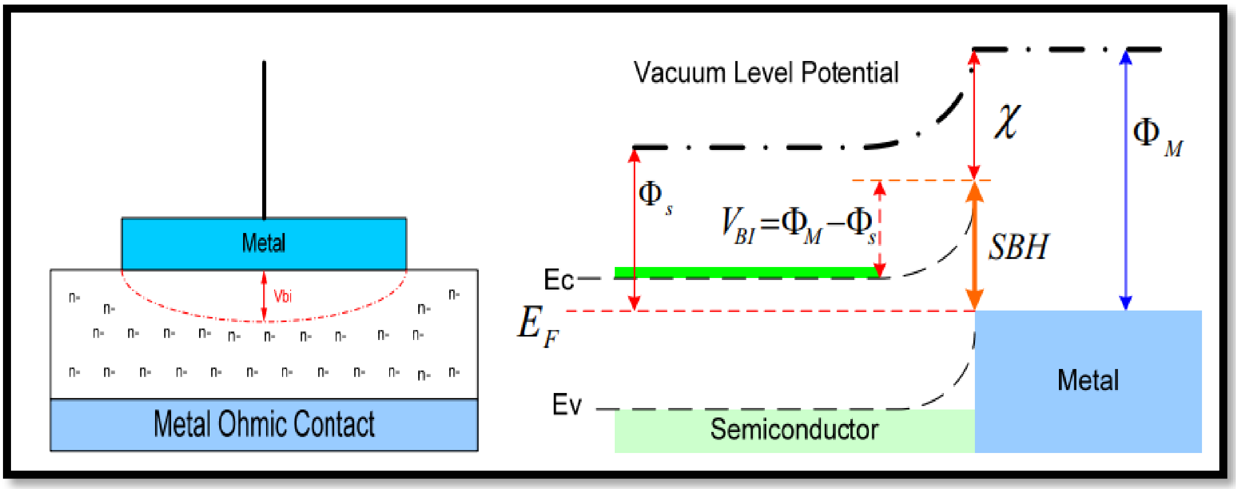

Figure1. 3: Metal and semiconductor in contact; band diagram of built-in potential.

The built-in potential V_{BI} also referred to as equilibrium contact potential (occurring when the Fermi levels have reached a balance) is the mechanism that prevents any further charge movement from the semiconductor conduction band to the metal. This built-in potential V_{BI} is the difference in the work function of the metal and the work function of the semiconductor.

$$V_{BI} = \Phi_m - \Phi_s \qquad (1.3)$$

Schottky diodes are important electronic components, used in many applications such as solar cells, photodetectors and clamped transistors.

2.3 The principle of operation of a solar cell (photovoltaic):

The term “photovoltaic”, often abbreviated by the acronym “PV”, was formed from the words “photo” a Greek word meaning light and “Volta” the name of the Italian physicist Alessandro Volta who invented the electrochemical cell in 1800. The photovoltaic effect is the direct conversion of energy solar to electricity [7] , This transformation is based on the following three mechanisms:

- Absorption of photons (whose energy is greater than the gap).
- Conversion of the energy of the photon into electrical energy, which corresponds to the creation of electron / hole pairs in the semiconductor material.
- Collection of particles generated in the cell [8].

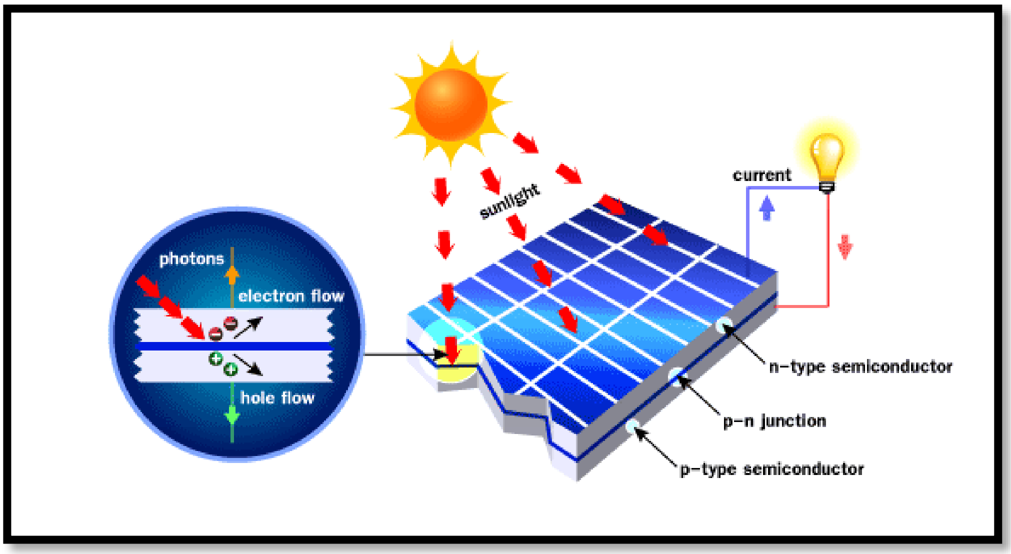

Figure1.4: principle of operation of a solar cell

The incident photons create carriers in the N and P zones and in the space charge zone. Photo carriers will behave differently depending on the region:

In the N or P zone, the minority carriers which reach the space charge zone, are sent by the electric field in the P zone (for the holes) or in the N zone (for the electrons) where they will be the majority. We will have a diffusion photo-current.

In the space charge zone, the electron / hole pairs created by the incident photons are dissociated by the electric field: the electrons will go towards the N region, the holes towards the P region[8].

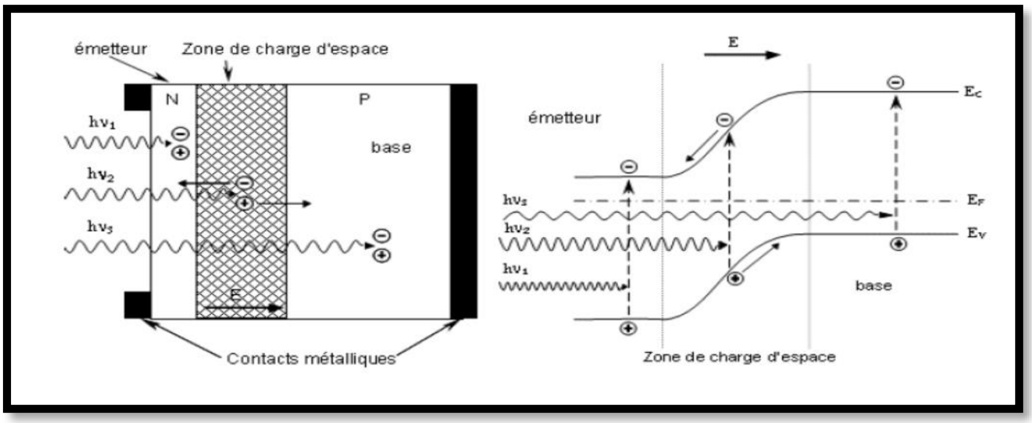

Figure1.5: structure (left) and band diagram (right) of a photovoltaic cell

2.4 Basic semiconductor device equations

The semiconductor device equations can be used to describe the whole simulation domain of a semiconductor device.

2.4.1 Poisson's Equation

$$-\frac{d^2\varphi}{dx^2} = \frac{dE}{dx} = \frac{Q}{\varepsilon_0 \varepsilon} \qquad (1.\ 4)$$

$$\frac{dE}{dx} = \frac{q}{\varepsilon_0 \varepsilon}(p - n + N_D^+ - N_A^-) \qquad (1.\ 5)$$

Where:

φ is the electrostatic potential

ε0 is the permittivity of free space

ε is the static relative permittivity of the medium

2.4.2 The Current Density Equations

For the electrons:

$$I_n = q\left(n\mu_n E + D_n \frac{dn}{dx}\right) \qquad (1.\ 6)$$

For the holes:

$$I_p = q\left(p\mu_p\ E + D_p\ \frac{dp}{dx}\right) \qquad (1.\ 7)$$

Where

n and p are electron and hole densities,

μn and μp are the electron and hole mobilities

Dn and Dp are the electron and hole diffusion constants

.

2.4.3 The diffusion current Equations

The diffusion current of both electrons and holes is given by:

$$J_n(x) = qD_n \frac{dn(x)}{dx} + q\mu_n n(x)E(x) \qquad (1.\ 8)$$

$$J_p(x) = -qD_p \frac{dp(x)}{dx} + q\mu_p\ p(x)E(x) \qquad (1.\ 9)$$

2.4.4 The Continuity Equations

$$0 = \frac{1}{q}\frac{dJ_n(x)}{dx} + G_n(x) - R_n(x\ ) \qquad (1\ .10)$$

$$0 = \frac{1}{q}\frac{dJ_p(x)}{dx} + G_p(x) - R_p(x) \qquad (1.\ 11)$$

Substituting (1.8) and (1.9) in (1.10) and (1.11) respectively we get:

$$0 = \mu_n n \frac{dE(x)}{dx} + \mu_n E \frac{dn(x)}{dx} + D_n \frac{d^2 n(x)}{dx^2} + G_n(x) - R_n(x) \quad (1.\ 12)$$

$$0 = \mu_p\, p\, \frac{dE(x)}{dx} + \mu_p\, E \frac{dp(x)}{dx} + D_p \frac{d^2 p(x)}{dx} + G_p(x) - R_p(x) \quad (1.13)$$

Where:

R(x) are the position-dependent volume recombination and

G(x) are photo generation rates [9]

2.5 History of solar cells

1839: Alexandre Edmond Becquerel observes the photovoltaic effect via an electrode in a conductive solution exposed to ligh [10]

1877 :W.G. Adams and R.E. Day observed the photovoltaic effect in solidified selenium, and published a paper on the selenium cell [11]

1905: Albert Einstein publishes a paper explaining the photoelectric effect on a quantum basis [12]

1931:A. H. Wilson develops theory of high purity semiconductor [13].

1948: Gordon Teal and John Little adapt the Czochralski method of crystal growth to produce single-crystalline germanium and, later, silicon [14]

1976: David Carlson and Christopher Wronski of RCA laboratories create first amorphous silicon PV cells, which have an efficiency of 1.1 %   [15]

1990:L. Fraas, J. Gee, K. Emery, et al. describe the 35 % efficient two-chip stack GaAs/GaSb concentrator solar cell [16]

1995: Grid-connected photovoltaic roof programs were launched in Japan and Germany and have been widespread since 2001[17]

2.6 The three generations of solar cells

2.6.1 First Generation

The photovoltaic industry is 90% focused on the use of silicon as a base material , This semiconductor has different advantages: it is abundant on the surface of the globe because easily extracted from the sand [18]. The technology of this generation is mature and well mastered for its two monocrystalline and multicrystalline types. The efficiency of silicon solar cells lies between 15-26 % [19]

Table1.1: 1st generation solar cells [20]

Classification	Efficiency (%)	Area (cm^2)	Test centre (date)
Si (monocrystalline cell)	26.3 ± 0.5	180.43	FhG-ISE (7/16)
Si (multicrystalline cell)	21.3 ± 0.4	242.74	FhG-ISE (11/15)

FhG-ISE : Fraunhofer Institut für Solare Energiesysteme

2.6.2 Second Generation

These technology do hold promise of higher efficiencies and offer cheaper production costs. However, the production stages require more energy because vacuum processes and high-temperature treatments are used.

It concerns thin-film solar cells with a thickness of less than 50 μm, The most successful second-generation materials are cadmium telluride (CdTe), copper indium gallium selenide, amorphous silicon and micromorphous silicon , [18, 21]

Table1.2: 2nd generation solar cells [20]

Classification	Efficiency (%)	Area (cm2)	Test centre (date)
GaAs	28.8 ± 0.9	0.9927	NREL (05/2012)
CIGS	21.0 ± 0.6	0.9927	FhG-ISE (04/2014)
CdTe	21.0 ± 0.4	1.0623	Newport (08/2014)
amorphous silicon	10.2 ± 0.3	1.001	AIST (07/2014)
micromorphous silicon	11.8 ± 0.3	1.044	AIST (10/14)

AIST: Japanese National Institute of Advanced Industrial Science and Technology

NREL: National Renewable Energy Laboratory.

2.6.3 Third Generation

This generation is based on the variety of new materials except silicon, most of the work on 3rd generation solar cells is carried out in the laboratory The goal of course is to improve the solar cells by making solar energy more efficient over a wider band of solar energy , This generation of solar cells includes dye-sensitized solar cells, perovskite solar cells and organic thin film [19] .

Table1.3: 3rd generation solar cells [20]

Classification	Efficiency (%)	Area (cm2)	Test centre (date)
Dye (cell)	11.9 ± 0.4	1.005	AIST (09/2012)
Organic (cell)	11.2 ± 0.3	0.992	AIST (10/2015)
InGaP/GaAs/InGaAs (Multijunction)	37.9 ± 1.2	1.047	AIST (02/2013)
Perovskite/Si (monolithic)	23.6 ± 0.6	0.990	NREL (08/2016)
GaInP/GaAs; GaInAsP/GaInAs	46.0 ± 2.2	0.0520	AIST (10/2014)

2.7 Solar Cell Characteristics

PV cells are usually characterised with four performances: short circuit current Isc, open circuit voltage Voc, fill factor FF, and conversion efficiency η.

figure 6: represents a characteristic voltage-current I(V) in the dark and under typical illumination of a photovoltaic cell with PN junction .

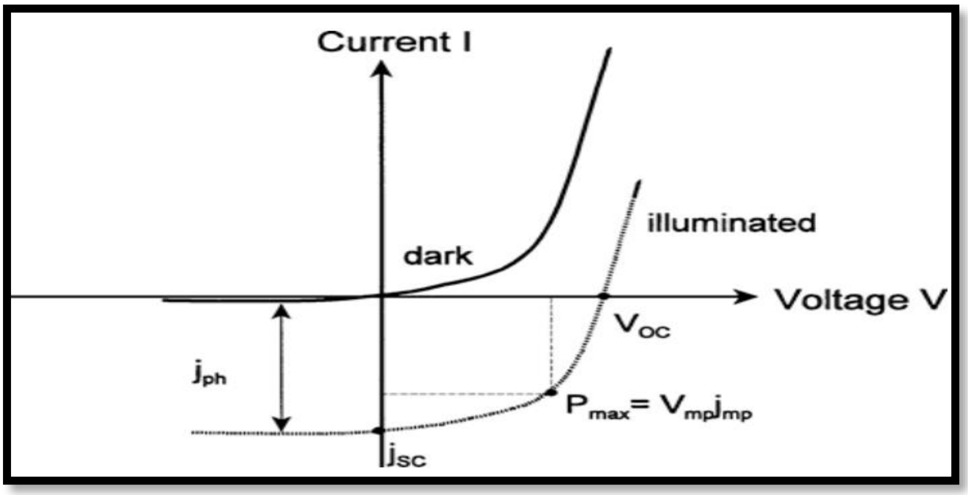

Figur1.6: Current-voltage characteristics of a solar cell in dark and under illumination [22]

2.7.1 Short Circuit Current Isc

The short-circuit current is the current through the solar cell when the voltage across the solar cell is zero (i.e., V=0), It grows linearly with the illumination intensity of the cell and depends on the illuminated surface, the wavelength of the radiation, the mobility of the carriers and the temperature. In this case, the short circuit current can be considered to be equivalent to the photocurrent Iph [23]

$$\mathrm{Isc} = -I_{ph} \qquad (1\ .\ 14)$$

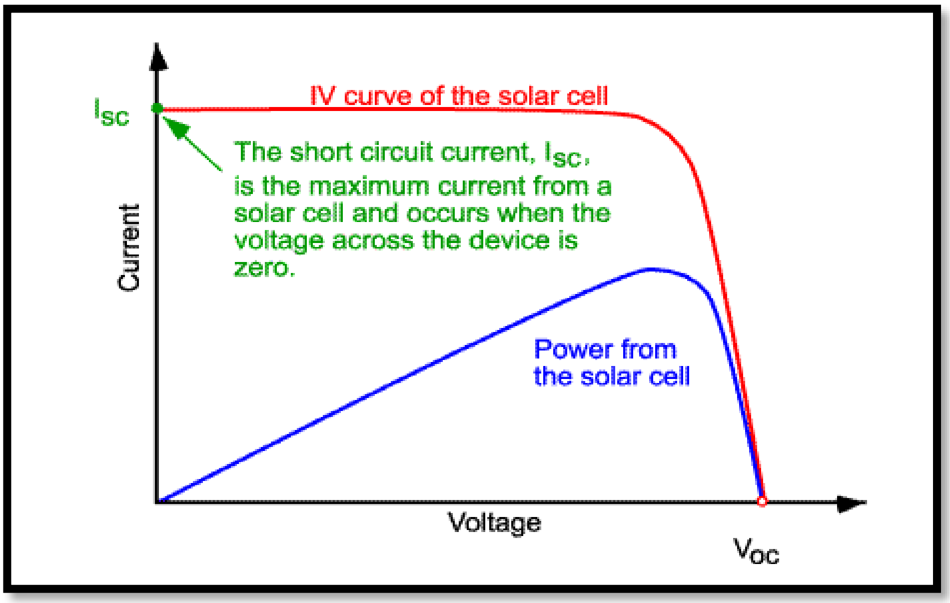

Figure 1.7: Short circuit current[24]

2.7.2 Open Circuit Voltage:

The open circuit voltage is the maximum possible voltage generated across the terminals of a solar cell when they are kept open, i.e., *I=0* It is given by the relation: [25]

$$V_{oc} = \frac{\eta K_B T}{q} \ln[(\frac{I_{ph}}{I_S}) + 1] \quad (1.15)$$

Where:

$\mathbf{I_{ph}}$ **:** Photo-generated current by the solar generator under illumination (A)

$\mathbf{I_s}$**:** Saturation current of the solar cell(A)

$\mathbf{K_B}$**:** Boltzmann constant and equal $1.38 \times 10{-}23$ *J/K*

η : Ideal factor of the solar cell

T: Temperature(K)

q: Electric charge(C)

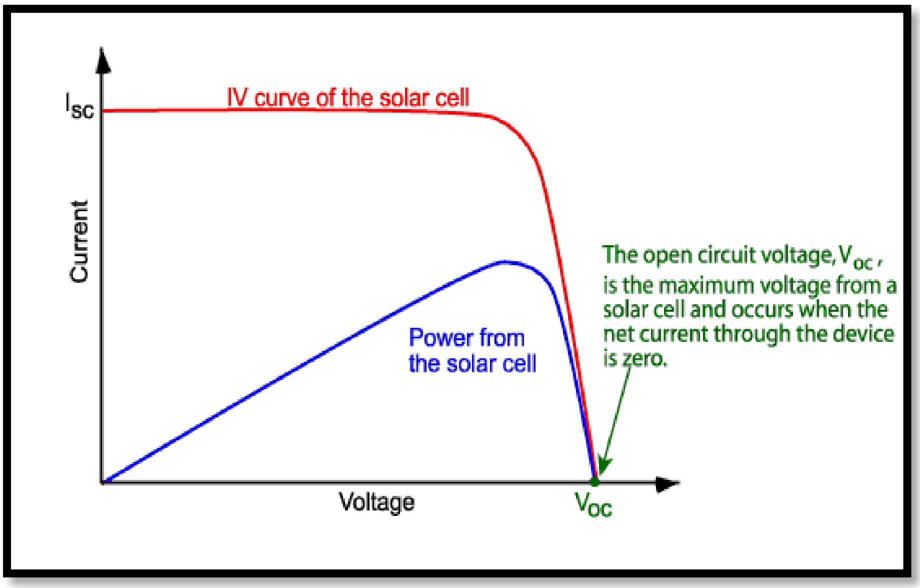

Figure1. 8: Open circuit voltage [24]

2.7.3 Fill Factor FF:

The FF is a key parameter in evaluating the performance of solar cells. It is represented in terms of percentage, it is defined as the ratio of maximum power $P_m = V_m . I_m$ that can be extracted from a solar cell to the ideal power $P_0 = V_{oc}.I_{sc}$. The following relation gives the FF [21] :

$$FF = \frac{P_m}{V_{oc}.I_{sc}} = \frac{V_m.I_m}{V_{oc}.I_{sc}} \qquad (1.\ 16)$$

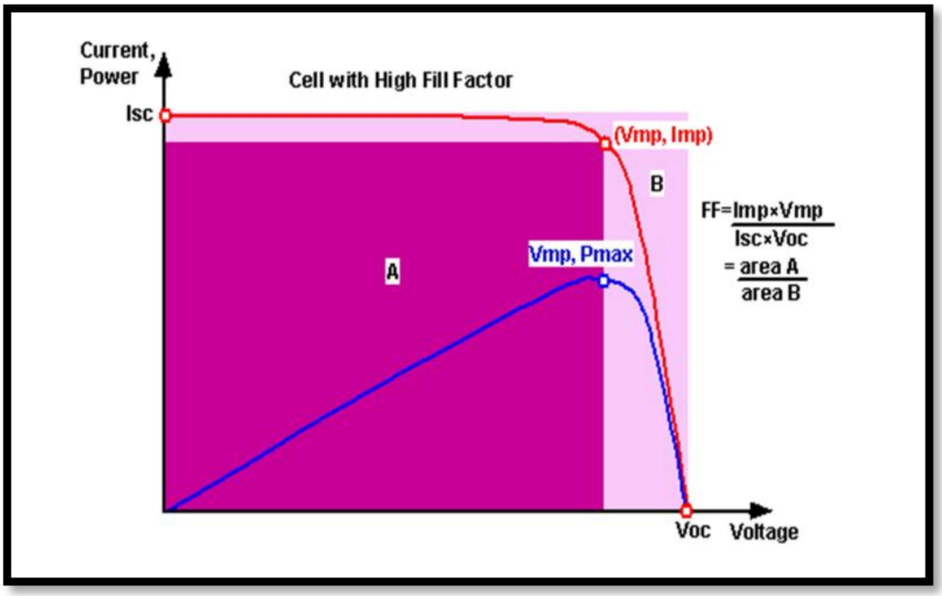

Figure1.9: The Fill Factor FF[24]

2.7.4 Efficiency:

The efficiency is the most commonly used parameter to compare the performance of one solar cell to another. Efficiency is defined as the ratio of energy output from the solar cell to input energy from the sun. In addition to reflecting the performance of the solar cell itself, the efficiency depends on the spectrum and intensity of the incident sunlight and the temperature of the solar cell.

The efficiency of a solar cell is determined as the fraction of incident power which is converted to electricity and is defined as: [26]

$$\eta = \frac{P_{max}}{P_{in}} \times (100\%) = \frac{V_m.I_m}{P_{in}} \times (100\%) = \mathrm{FF} \times \frac{V_{oc}.I_{sc}}{P_{in}} \times (100\%) \quad (1.17)$$

Where:

$Pin = E \times S$

E: Intensity of illumination in W/Cm^2

S: The area of the solar cell.

2.8 Solar cell applications:

Table 1.4: Solar cell applications

Home	Indoor and outdoor lighting system, electrical equipment, electric gate opener, security system, ventilator, water pump, water filter and emergency light
Lighting system	Bus stop lighting, telephone booth lighting, billboard lighting, parking lot lighting, indoor and outdoor lighting and street lighting
Water pumping	Consumption, public utility, livestock watering, agriculture, gardening and farming, mining and irrigation
Battery charging system	Emergency power system, battery charging center for rural village and power supply for household use and lighting in remote area
Agriculture	Water pumping, agricultural products fumigator, thrashing machines and water sprayer,
Cattle	Water pumping, oxygen filling system for fish-farming and insect trapped lighting
Health center	Refrigerator and cool box for keeping medicines and vaccines and medical equipment,
Communication	Air navigational aid, air warning light, lighthouse, beacon navigation aid, illuminated road sign, railway crossing sign, street lighting and emergency telephone
Telecommunication	Microwave repeater station, telecommunication equipment, portable communication equipment (e.g. communication radio for service and military exercise) and weather monitoring station
Remote area	Hill, island, forest and remote area that the utility grids are not available
Space	Satellite, international space station and spacecraft

2.9 Advantages and disadvantages of solar cell:

Photovoltaic energy has enormous advantages such as:

- Free access to this resource and the enormity of its potential spread across the globe .
- Cleanliness during use
- High reliability
- Low maintenance
- Great production flexibility (varying from milliwatts to megawatts)
- Autonomous and decentralized use

Despite these interesting advantages, there are also disadvantages such as:

- Diffuse source of solar radiation that requires large areas
- Expensive technology
- Low load factor
- Difficult storage
- Difficulty recycling system components
- High investment depending on political decisions [19]

Chapter 2: Graphene based solar cells

Chapter 2: Graphene based solar cells

1 Introduction

photovoltaic technology today is facing many obstacles; some of them are the limits of silicon and the conducting materials. the need for a new material is more than urgent to ensure the continuity of the technological development. to this point, 2D materials seem to be the perfect solution for this dilemma.

The use of graphene to improve the efficiency of solar cells is studied in this thesis. To understand how graphene-based solar cells work, we will present some concepts, including (graphene shapes, general principle of graphene synthesis, graphene production techniques, properties of graphene..) We will also discuss the use of graphene in solar cells and Graphene-based solar cells

2 Graphene

Graphene calls great interest throughout the international scientific community. The first person who described graphene was Hanns-Peter Boehm. In 1962, he characterized it as a carbon-dimensional structure observed by X-ray diffraction, while research on allotropic varieties atoms (observing the fine particles of graphite) [27], For the first time managed to isolate graphene in 2004 a group of British and Russian scientists Andre Geim and Konstantin Novoselov.

It is now known that graphene is composed of a single layer of carbon atoms forming the honeycomb structure (Fig.1) [28], It is made up entirely of carbon atoms bound together in a network of repeating hexagons within a single plane just one atom. The length of the bonds between the carbon atoms is about 0.0142 nm [29].

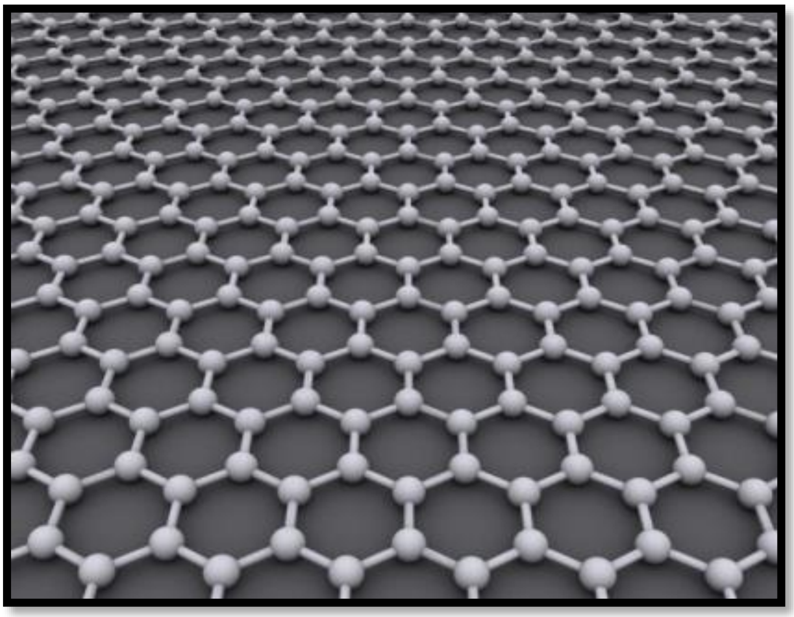

Figure2.1 : Structure of graphene

2.1 Forms of Graphene

2.1.1 Graphene Monolayer

It is a single atom-thick sheet of hexagonally arranged sp^2 - bonded carbon atoms which is freely suspended or adhered on a foreign substrate. Its lateral dimensions may vary from several nanometers to microscale. Monolayer (single-layer) is the purest form known and is useful for high-frequency electronics. Bi-layer and tri-layer Graphene, two and three layers respectively, exhibit different properties with the increase in the number of layers.

2.1.2 Few-Layer Graphene (FLG) or Multi-Layer Graphene (MLG)

They consist of a small number (between two to 10) well defined, countable, stacked Graphene layers of extended lateral dimension. They can be sheet-like, free-standing films or flakes or a substrate bounded coating. These are useful for composite materials, as a mechanical reinforcement.

2.1.3 Graphene Oxide (GO)

Graphene Oxide is a monolayer material with high oxygen content, where C/O atomic ratio is in between 2 – 3. It is prepared by oxidation and exfoliation that is followed by extensive oxidative modification of the basal plane. Thin membranes prepared using GO allow water to pass through but restrict harmful gases.

2.1.4 Reduced Graphene Oxide (rGO)

It is Graphene oxide (as above) which is reductively processed by chemical, photo-chemical, thermal, photo-thermal microwave or microbial/bacterial methods to reduce its oxygen content.

2.1.5 Graphene nanomaterials

These include Graphene nanosheets, Graphene nanoribbons, Graphene nanoflakes, etc. They are broadly defined as two-dimensional Graphene materials with a thickness and/or lateral dimension of less than 100 nanometers. They are not an integral part of carbon material, but is freely suspended or adhered on a foreign substrate. They are perfect for electrically conductive composites [30].

2.2 General principle of graphene synthesis

The graphene synthesis is based on two general methodologies, bottom-up and top-down approaches, as shown in Figure 2. In the top-down method, starting material is graphite and the aim is to intercalate and exfoliate it to graphene sheets through solid state, liquid state or electrochemical exfoliations. Another approach in this category is to exfoliate graphite oxide to grapheme oxide (GO) followed by chemical or thermal reduction[31]. The bottom-up method is based on making graphene from molecular precursors building blocks by chemical vapor deposition (CVD) or epitaxial growth [32].

The structure, morphology and properties of the resulted graphene such as number of layers, defect level, electrical and thermal conductivity, solubility and hydrophilic or hydrophobicity depend on the fabrication method

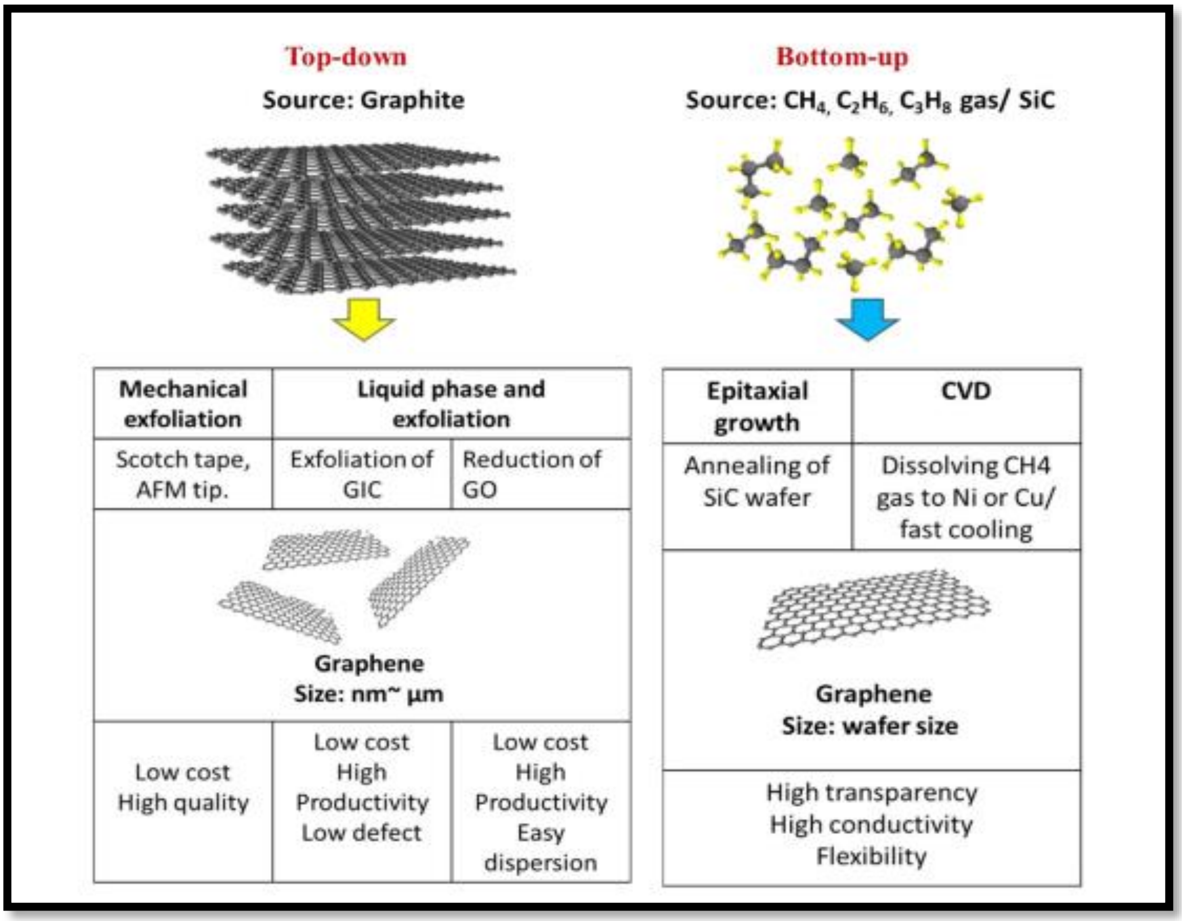

Figure2. 2: Schematic of top-down and bottom-up approaches for graphene synthes [33]

2.3 Production techniques

Graphene can be produced using a variety of techniques ranging from simple to state-of-the-art technologies

2.3.1 Mechanical Exfoliation

This technique was first introduced by R. Ruoff and group [34].They used an adhesive tape to split the Graphene layer from graphite flakes. Multiple exfoliation steps are required to obtain single layers. After exfoliation these layers were deposited on a silicon wafer using 'dry deposition'. This technique is also known as 'Scotch tape' or 'drawing' method.

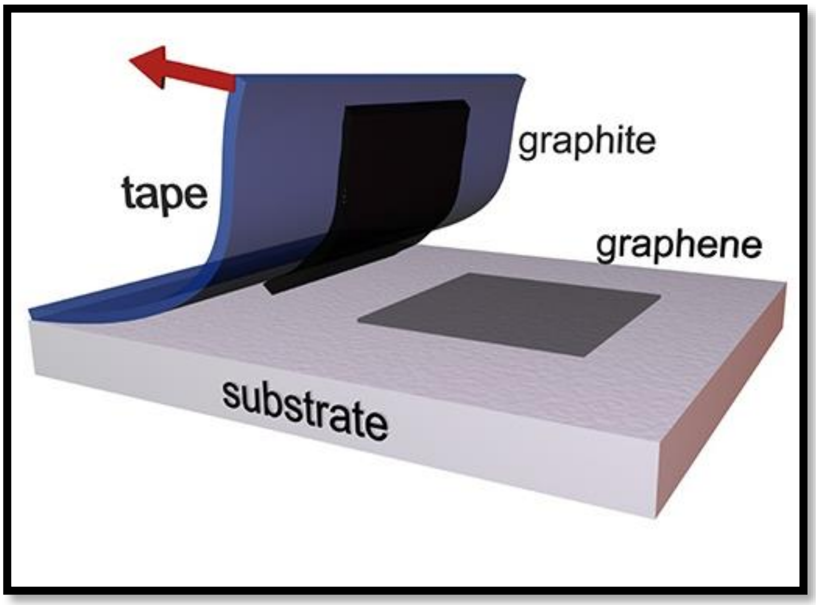

Figure2.3 : Picture of Mechanical Exfoliation [35]

2.3.2 Chemical vapor deposition (CVD)

Another well-known method is the preparation of graphene by chemical vapor deposition method (CVD) on metallic substrates (Cu, Ni, s Pt, Pd, Ru, Ir, Co itp.) , The most widely used metal today for the quality of the graphene produced, the financial cost and the mechanical properties is copper[36].

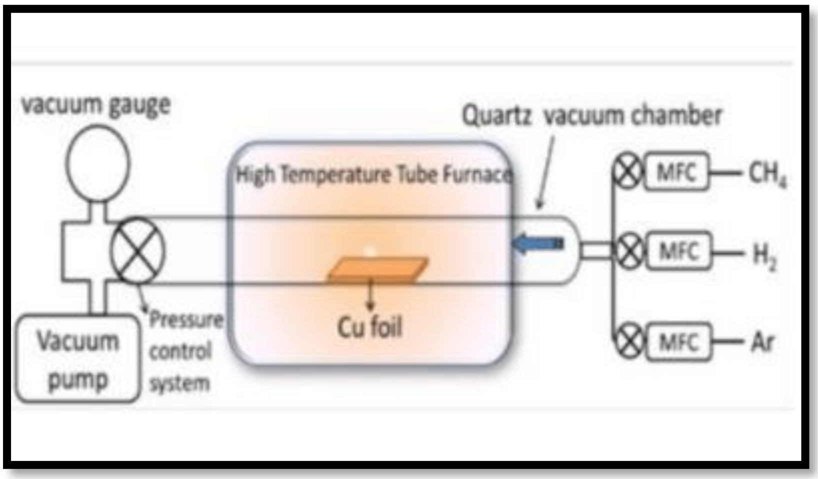

Figure2.4 : Diagram of a CVD chamber[37]

To synthesize graphene, it is necessary to bombard the surface of the copper which is heated to a high temperature, around 1000 ° C, with the help of hydrocarbon gases which will decompose on the surface into single carbon atoms and a gaseous residue of the a decomposition of gas. Several types of gas are used for this, but the most common are methane, acetylene or ethylene[35].

2.3.3 Electrochemical mechanisms of exfoliation

The electrochemical setup that is used to exfoliate graphite normally contains the following elements: a graphite working electrode, counter electrode, reference electrode, electrolyte, and power supply[38]. The working electrode and counter electrode are immersed into electrolyte with a certain distance kept between them. Positive or negative voltage is applied to the graphite working electrode depending on the exfoliation mechanism desired [39]

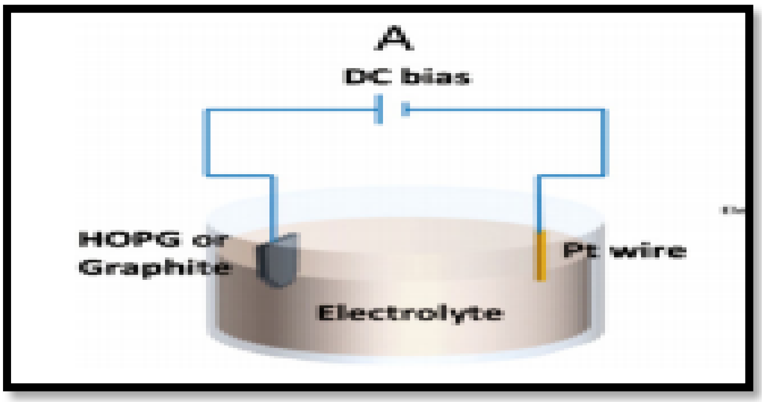

Figure2. 5: Schematic illustration of a typical setup for the electrochemical exfoliation of graphite [39]

2.3.4 Chemically derived Graphene from Graphite Oxide

This method involves production of graphite oxide from graphite and then the synthesis of Graphene [40] , Graphite is chemically modified into a water dispersible intermediary graphite oxide by oxidizing using Hummers' method[30].

The biggest advantage of this method is its low-cost and enormous scalability.

2.4 Graphene properties

Many researchers have reported record-breaking electronic, mechanical and optical properties of Graphene, which may make it a material of great utility

2.4.1 Electronic Properties

Graphene has very high electrical conductivity as it is a zero gap semi-conductor, because its conduction and valance bands meet at the Dirac points[41].

Electronic mobility of Graphene is very high even at room temperature. It has been experimentally proven that it electron mobility is nearly independent of temperature[42] .

2.4.2 Mechanical Propertie

According to Changgu Lee, Graphene is the strongest material ever tested, with a Tensile strength of 130 GPa and a Young's Modulus (defines stiffness) of 1 TPa, Apart from this, it is unbelievably light, weighing about only 0.77 mg/m^2 [43, 44].

2.4.3 Optical Properties

Graphene produces a highly opaque atomic monolayer in vaccum, as it has an ability to absorb approximately 2.3% of the white light. Therefore, it is considered a transparent material and its transparency is estimated to be 97.7% [45].

2.4.4 Thermal properties

The thermal conductivity of single-layer suspended graphene at room temperature has been measured as 3000–5000 W m1 K1 depending on the size of the measured graphene sheet. Nevertheless, this value is still about 2 times and 50 times higher than copper and silicon, respectively, which are used in the electronics today[46] .

3 Silicon

3.1 Definition

Silicon (Si), a nonmetallic chemical element in the carbon family (Group 14 [IVa] of the periodic table). Silicon makes up 27.7 % of Earth's crust;

The name silicon derives from the Latin silex or silicis, meaning "flint" or "hard stone." Pure silicon is too reactive to be found in nature, but it is found in practically all rocks as well as in sand, clays, and soils, combined either with oxygen as silica (SiO_2, silicon dioxide) or with oxygen and other elements (e.g., aluminum, magnesium, calcium, sodium, potassium, or iron) as silicates. The oxidized form, as silicon dioxide and particularly as silicates, is also common in Earth's crust and is an important component of Earth's mantle. Its compounds also occur in all natural waters, in the atmosphere (as siliceous dust), in many plants, and in the skeletons, tissues, and body fluids of some animals [47] .

Silicon's atomic structure makes it an extremely important semicoductor, and silicon is the most important semiconductor in the electronics and technology sector.

3.2 Silicon properties

Table2. 1 : Silicon properties [49]

Crystal structure	Face-centered diamond-cubic
Density	2.3290 g/cm^3
Melting point	1687 K
Thermal expansion	2.6 µm/(m·K)
Thermal conductivity	149 W/(m·K)
Electrical resistivity	2.3×10^3 Ω·m
Band gap	1.12 eV
Shear modulus	51–80 GPa
Young's modulus	130–188 GPa [48]

3.3 Types of silicon

Silicon used for solar cells can be single crystalline, multicrystalline, polycrystalline or amorphous. The key difference between these materials is the degree to which the semiconductor has a regular, perfectly ordered crystal structure, and therefore semiconductor material may be classified according to the size of the crystals making up the material.

4 Using graphene in solar cells

4.1 The use of graphene to exploit raindrops

The state-of-the-art solar cells can only be driven by sunlight on sunny days, while the solar-to-electric conversion efficiency is zero at night and nearly zero at other dark conditions such as rainy atmosphere. One of the solutions to this impasse is to create all weather solar cells that can be triggered by multiple stimuli according to rational design of functional components and charge transportation. To address this issue, a flexible solar cells have been developed to produce electricity by simulated sun and rain, in which graphene film is hot-pressed onto the back side (insulating polymer) of indium tin oxide/polyethylene terephthalate (ITO/PET) plastic substrate, while solar cell is built on ITO layer. Real raindrops are not pure water, they contain salts that split into positively and negatively charged ions When dropping the raindrops onto graphene surface, the raindrops spread quickly to the periphery, forming π-electron/cation electric double-layer (EDL) pseudocapacitors at graphene/raindrop interface and dragging electron migration and charging at the front of the droplets. The raindrops can shrink rapidly on graphene surface, releasing the electrons to graphene and discharging the pseudocapacitor . The charging-discharging processes can yield current and voltage signals under dropping of raindwater, yielding a maximal photoelectric conversion efficiency of 7.69%[50].

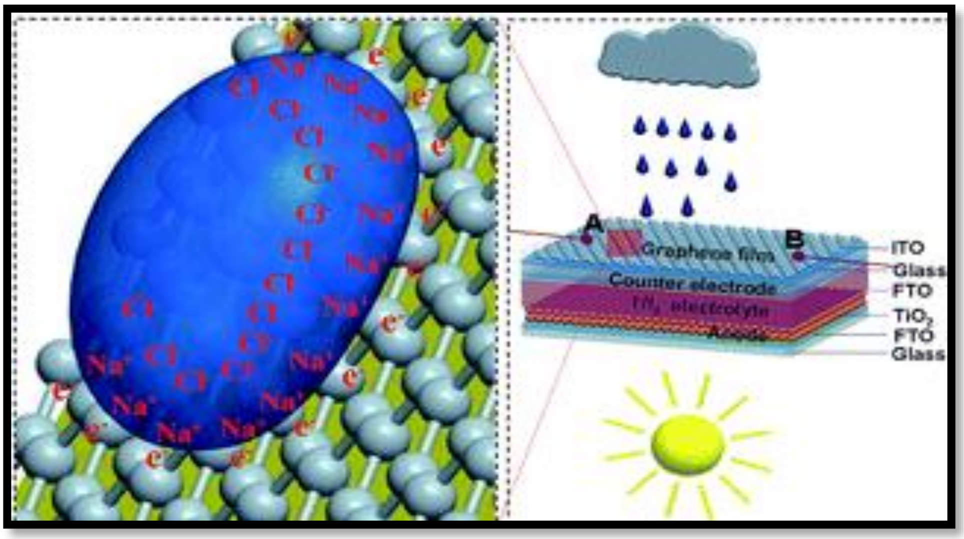

Figure2. 6 : Schematic illustrates of the bifunctional solar cells by covering [50]

4.2 The use of graphene as an electrode:

Graphene has attracted tremendous interest due to its unique physical and chemical properties. The atomic thickness, high carrier mobility and transparency make graphene an ideal electrode material which can be applied to various optoelectronic devices such as solar cells, light-emitting diodes and photodetectors. In recent years, there has been a growing interest in developing graphene/silicon Schottky junction solar cells and the power conversion efficiency has reached up to 15.8%[51] .

5 Graphene-based solar cells

5.1 Graphene-Composited Thin Film Solar Cell

These cells are the second generation of solar photovoltaic panels, and this type of cell is divided into:

5.1.1 Graphene with CdTe

Transparent 28rapheme conducting films are successfully incorporated in thin-film CdTe solar cells as the front electrode. A four-layer 28rapheme film, deposited by an ambient pressure chemical vapor deposition (CVD) method, possesses a carrier mobility of 550 cm^2 V^{-1} s^{-1} and an optical transparency of 90.5% from 350–2200 nm, achieving an overall efficiency of 4.17% in the prototype device[52] .

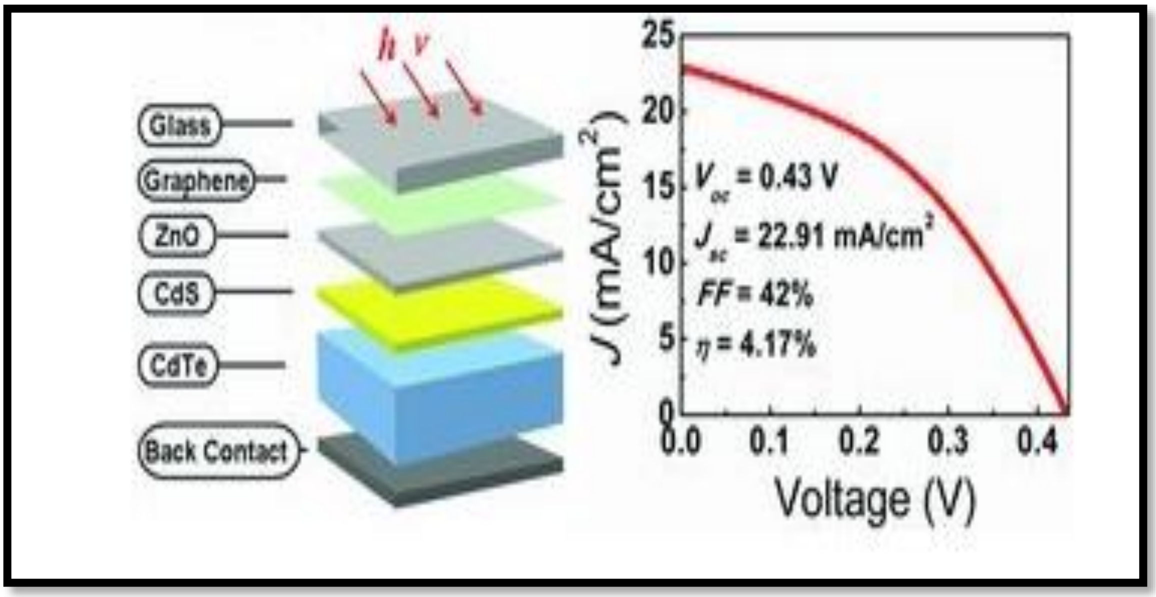

Figure 2.7: Schematic diagram and J–V characteristics of the glass/28rapheme/ZnO/CdS/CdTe/(graphite paste) solar cell [52]

5.1.2 Graphene with CIGS

Graphene films have been employed as window electrode in various thin film solar cells. However, to date graphene film has not been used as hole transport electrode, particularly in CIGS solar cell. we have demonstrated a novel structure for graphene-based flexible CIGS solar cell, in which graphene film on flexible Cu foil was implemented as hole transport electrode. CIGS solar cells were directly fabricated on the chemical vapor deposited graphene film on Cu foil, without any transfer process. Several techniques, including Raman spectroscopy, X-ray diffraction, scanning electron microscopy, external quantum efficiency and J-V characteristics under illumination, have been used to investigate the device performance. The graphene-based device displayed power conversion efficiency of 9.91 ± 0.89% with a fill factor of 64.75 ± 7.34%, which are substantially higher compared to reference cell fabricated using conventional Mo/stainless steel electrode. High open circuit voltage together with substantially large fill factor is primarily responsible for high cell efficiency of graphene/Cu foil based device[53].

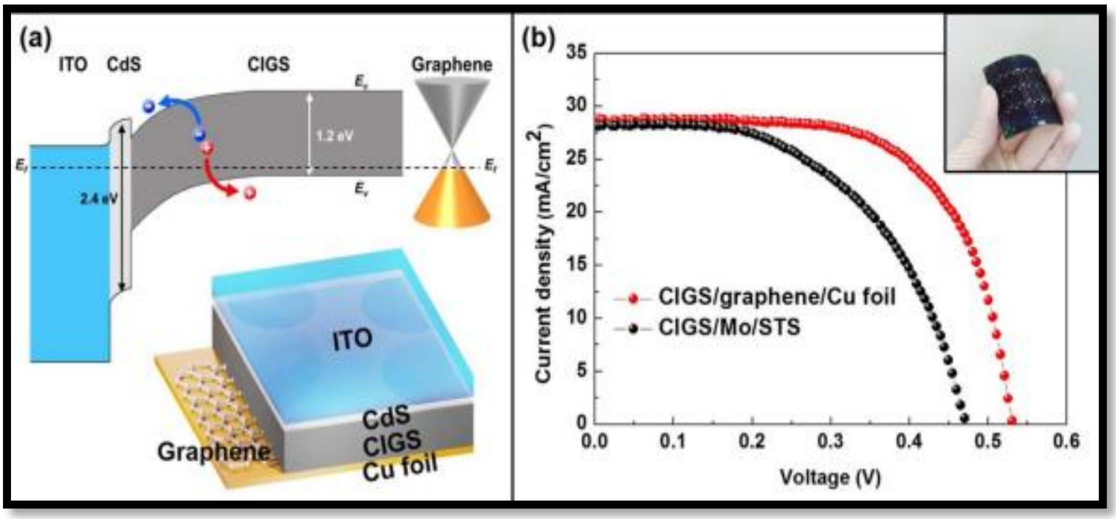

Figure2. 8: (a) Schematic design of the CIGS solar cells (b) J - V characteristics of the CIGS solar cell[53] .

5.2 Perovskite Solar Cells with Graphene

In summary, semitransparent perovskite solar cells were fabricated by laminating stacked the chemical vapor deposition (CVD) graphene as top transparent electrodes on perovskite layers for the first time. The devices with double-layer graphene electrodes show the maximum power conversion efficiencies (PCEs) of 12.02% ± 0.32% and 11.65% ± 0.35% from the fluorine-doped tin oxide (FTO) and graphene sides, respectively, which are relatively high compared with the reported semitransparent perovskite solar cells. graphene is an ideal candidate for transparent electrodes of perovskite solar cells. Considering its excellent mechanical flexibility and convenient preparation, graphene electrodes are expected to be used in fl exible perovskite solar cells by printing or roll to roll process, which may fi nd applications to complement the rigid inorganic solar cells currently dominated in the market[54].

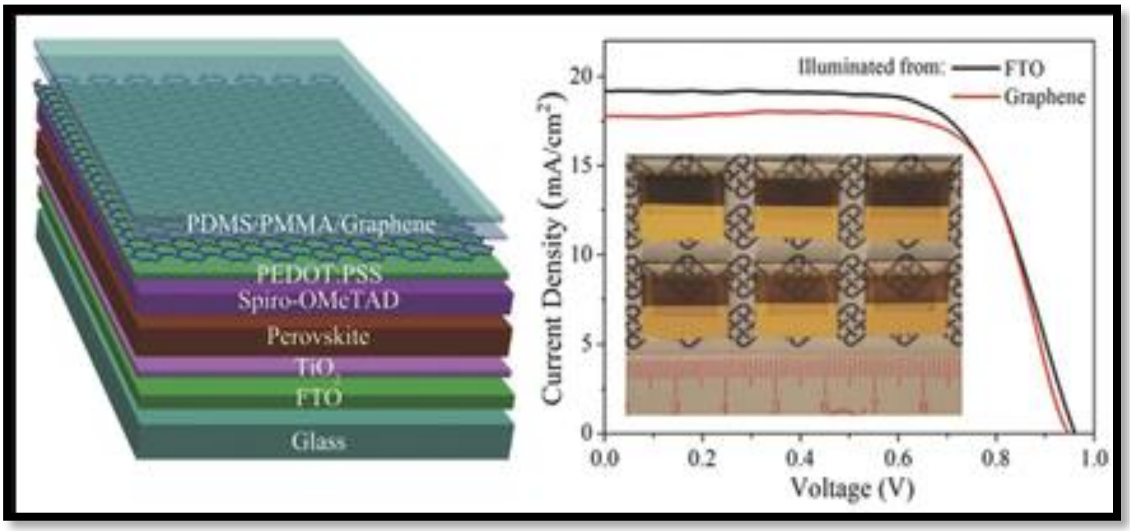

Figure 2.9: Schematic diagram of a semitransparent perovskite solar cell and . J – V characteristics of the semitransparent solar cells illuminated from the FTO side and the graphene side[54].

5.3 Graphene on Dye-Sensitized Solar Cells

In this type, a simple approach without a prereduction of graphene oxide was exploited to prepare a graphene-doped TiO_2 film for dye-sensitized solar cells (DSSCs). The performance measurement of the DSSCs showed that the incorporation of graphene could increase the short-circuit current density and power conversion efficiency by 52.4 and 55.3%, respectively. Furthermore, it was demonstrated that the performance enhancement was due to the promoting effect of graphene on electron transfer instead of the increase of dye loading in TiO_2/graphene composite films. However, graphene can also absorb solar light, which could lead to the decrease of light harvest of dye molecules and thus a negative effect on the power conversion efficiency of DSSCs. Furthermore, graphene might decrease the actual dye loading on TiO_2 in a TiO_2/graphene film, which can also make a negative contribution to the conversion efficiency. As a result, the promoting effect of graphene is strongly dependent on its content; namely, the efficiency of DSSCs increases to the maximum value and then decreases with increasing graphene content in TiO_2/graphene composites[55].

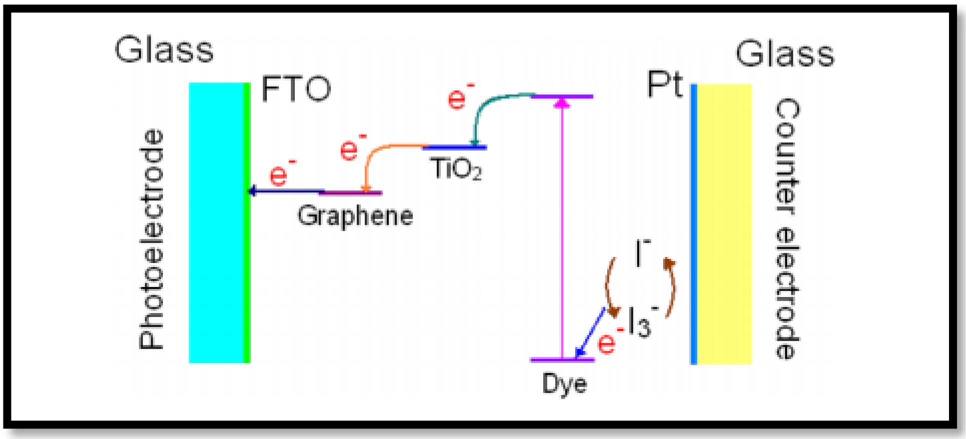

Figure 2.10: Principle scheme of TiO2/graphene-based DSSC

6 Graphene/Si Schottky solar cells :

In consideration the excellent optical and electrical properties of graphene, there is a great interest in developing graphene/Si Schottky junction solar cells in recent years. In 2010, the first graphene/n-Si Schottky junction solar cell was reported by Zhu *et al.* They showed that graphene film can be combined with Si to form efficient solar cells. In this kind of solar cells, graphene not only acts as a transparency electrode, but also plays an important role in photo-carriers separation and transport [56] The PCE of the graphene/Si solar cells has reached up to 15.8% in just a few years .

The structure of graphene/Si solar cells is illustrated in (Figure 11-a) The SiO_2 layer is wet-etched with pure or buffered HF solution from Si wafer to expose a square window which defines the active area of the solar cell. The front contact is prepared by photolithography and metal deposition, then single layer, bilayer or multilayer graphene is directly transferred onto the top of the patterned substrates *via* a solution method to create a conformal coating with the front contact and underlying n-Si. In such devices, a built-in electric field is established due to work function difference of the two materials, graphene and n-type Si adjust their Fermi lever to the common position (Figure 11-b) [57] When incident light penetrate into the junction, the electron–hole pairs are created in Si and then carriers are separated by the built-in electric field. The electrons drift toward the n-type Si direction and holes drift to the graphene side, resulting in the output of current and power. In graphene/Si solar cells, the built-in potential Φ_{SBH} is determined by the difference between the work function of graphene Φ_G and the electron affinity of n-Si χ_{Si} [58] .

Since the work function of graphene is tunable, we have more freedom in device design to optimize the separation and collection of the electrons and holes in graphene/Si solar cells, and result in larger potential drop across the depletion width, all of which can allow a more efficient collection of carriers.

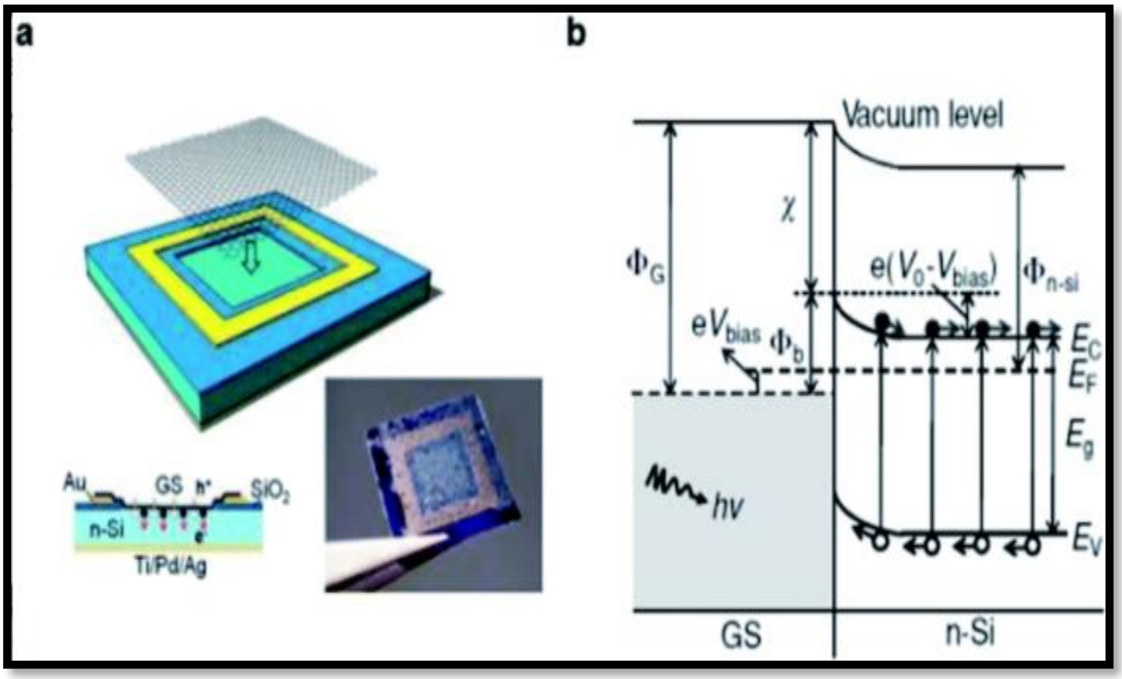

Figure 2.11: Characterizations of the graphene/n-Si Schottky junction. **(a)** Schematic illustration of the device configuration. **(b)** Energy diagram of the forward-biased graphene/n-Si Schottky junction upon illumination.

Chapter 3:

SILVACO simulation and results

Chapter 3:SILVACO simulation and results

1 Introduction

In our work, we used technological simulation software SILVACO (TCAD), to simulate the electrical and optical characteristics of a Schottky junction Graphene/Si solar cell. First, we should learn some basic notions about simulation in general and this software and particularly using examples illustrating the work, and then we would proceed to our simulation and discuss the results that we obtained from our work.

The Role of Simulation The simulation offers a link between the experimental world and the theoretical one, as it complements theory and experiment and builds physical reality in the presence of certain constraints or the presence of an impossible mathematical analysis.

2 Silvaco Atlas Simulation Software

Silvaco's ATLAS software provides general capabilities for physically based two and three-dimensional simulation of semiconductor devices. ATLAS is used via DeckBuild, an interactive runtime environment. Figures can be made from the data obtained from the simulation and plotted using TONYPLOT, the included interactive graphics and analysis package. ATLAS has a comprehensive collection of physical models that are of use for modeling solar cells[59].

The ATLAS defined solar cell structure and composition requires several parameters to be defined. These basic parameters include a two-dimensional, fine division of the overall material called a mesh, the division of that mesh into regions, the assignment of materials to each region. Next, the electrode locations must be defined. Then, doping must be introduced into the respective materials. Also, a specification of a light spectrum for simulation must be made. The next step for the user is to choose among different models, finding that which is most the suitable for evaluating the structure, and achieving a better outline for the specific cell simulation.

2.1 Atlas operation mode

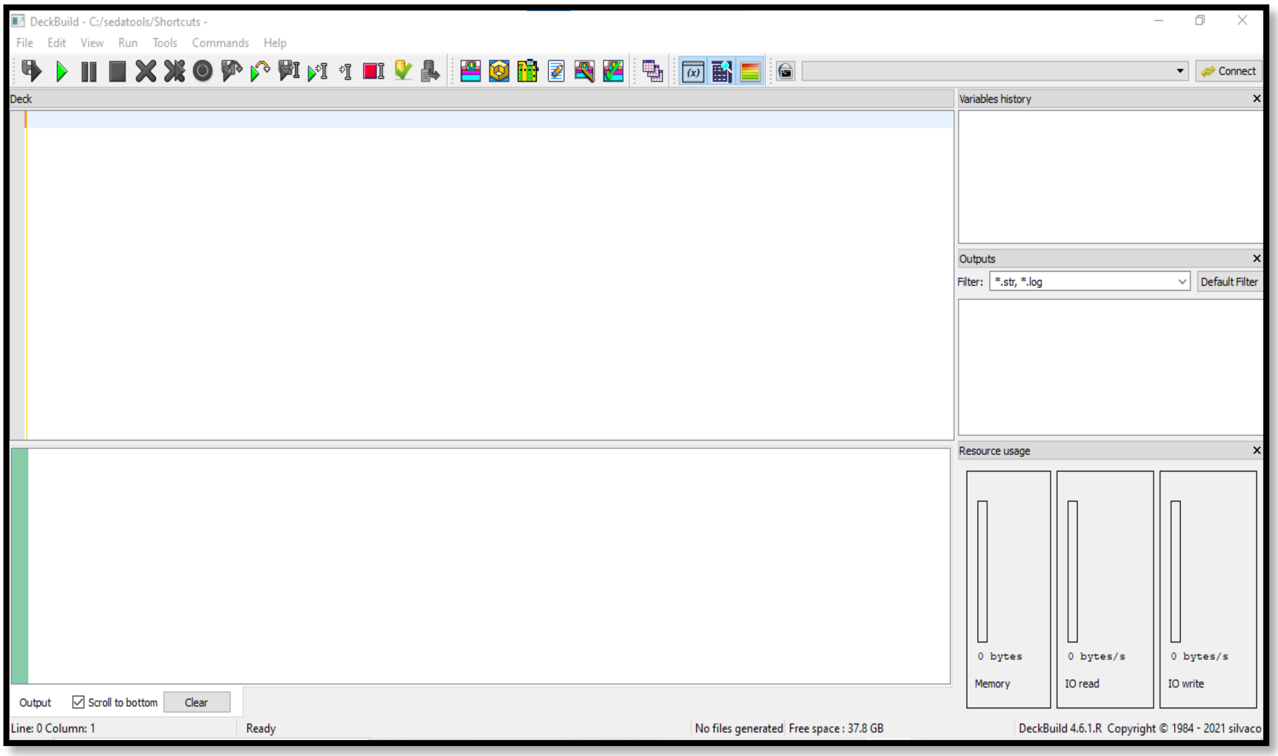

Figure 3.1: DECKBUILD window

The command is entered in DECKBUILD by go atlas like the picture shown above.

The Order of Atlas commands in which the statements appear in the Atlas input file is important. There are five sets of statements that must occur in the correct order or else an error message will appear, which may cause incorrect start or termination must occur in the correct order or else an error message will appear, which may cause incorrect start or termination of the program. For example, if the material parameters or models are set in the wrong order, then they may not be used in the calculations.

The order of statements within the mesh definition, structural definition, and solution groups is also important. Otherwise, it may also cause incorrect operation or termination of the program.

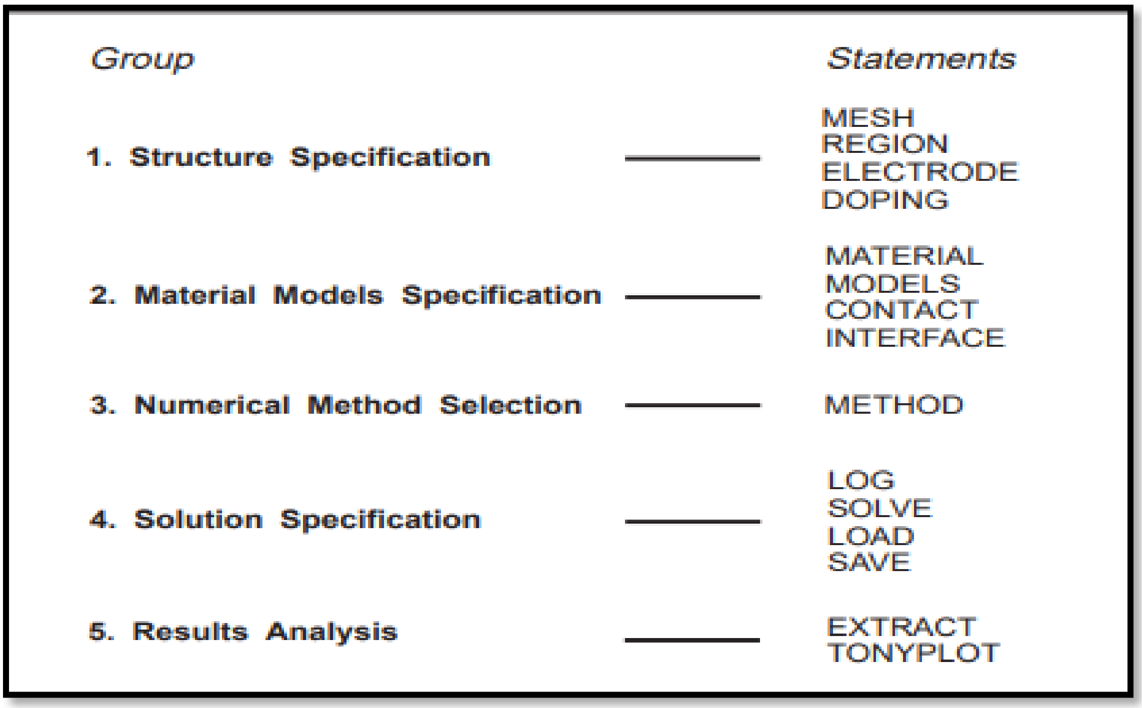

Figure 3.2: ATLAS Command Groups with the Primary Statements in each Group [60]

2 .2 Structure Specification

The structure specification is done by defining the mesh, the region, the electrodes and the doping levels

2.2.1 Mesh

The first section of structure defining statements in the Deckbuild program is the meshing section. this section specifies the two dimensional grid that is applied to the device with mesh statements.

The following instruction is used to define the meshing:

MESH SPACE.MULT=<VALUE>

X.MESH LOCATION=<VALUE> SPACING=<VALUE>

Y.MESH LOCATION=<VALUE> SPACING=<VALUE>

The Atlas device simulator can more easily solve the differential equations at each grid point if there are no abrupt changes between adjacent points. Mesh statements have two parts called location statements and spacing statements.

The location statement "loc" specifies the x or y value in the structure to which the following "spacing" statement is applied.

The spacing statement "space" specifies the spacing between grid lines at that specific location.

Figure.3, shows the mesh of the studied cell solar.

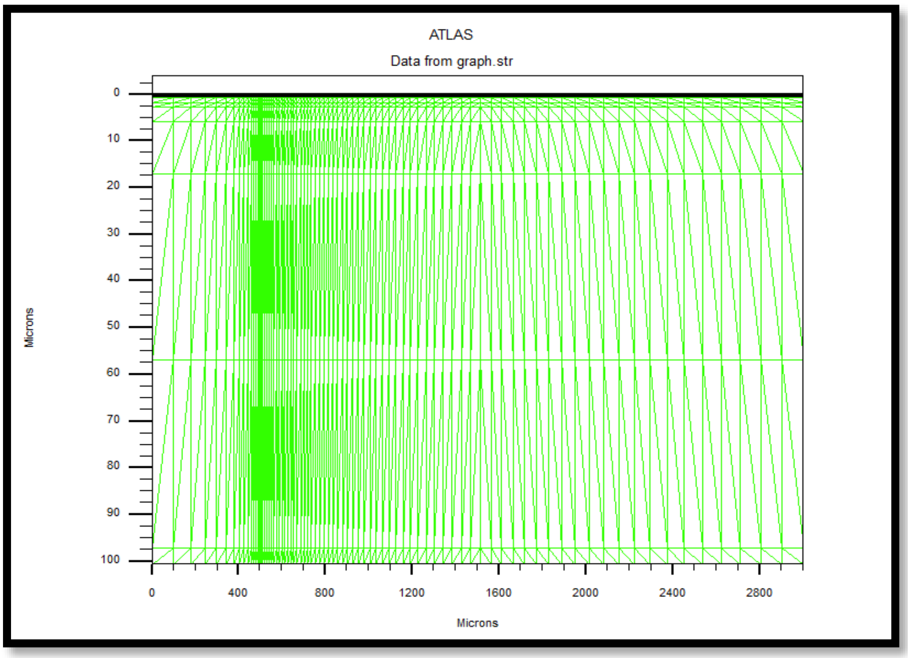

Figure 3.3: Atlas mesh

2.2.2 Region:

Once the mesh is specified, every part of it must be assigned a material type. This is done with REGION statements. For example

REGION number=<integer> <material_type> /<position parameters>

region number=1 material=silicon x.min=0.0 x.max=200 y.min=7.005 y.max=107.005

Every region must have a different number as the program produces an error if a statement applies to two different regions

The material specification statement specifies that the whole region consist of the stated material. This statement gives that whole region default parameters and characteristics of that specified material, which are stored in the ATLAS material library. These values include parameters such as the bandgap, electron and hole mobility, and optical properties such as the index of refraction. These parameters can be used or changed in another section of the structure defining code if the user wishes to modify a material's original properties.

Figure 3.4 shows regions generated by Atlas for the cell solar.

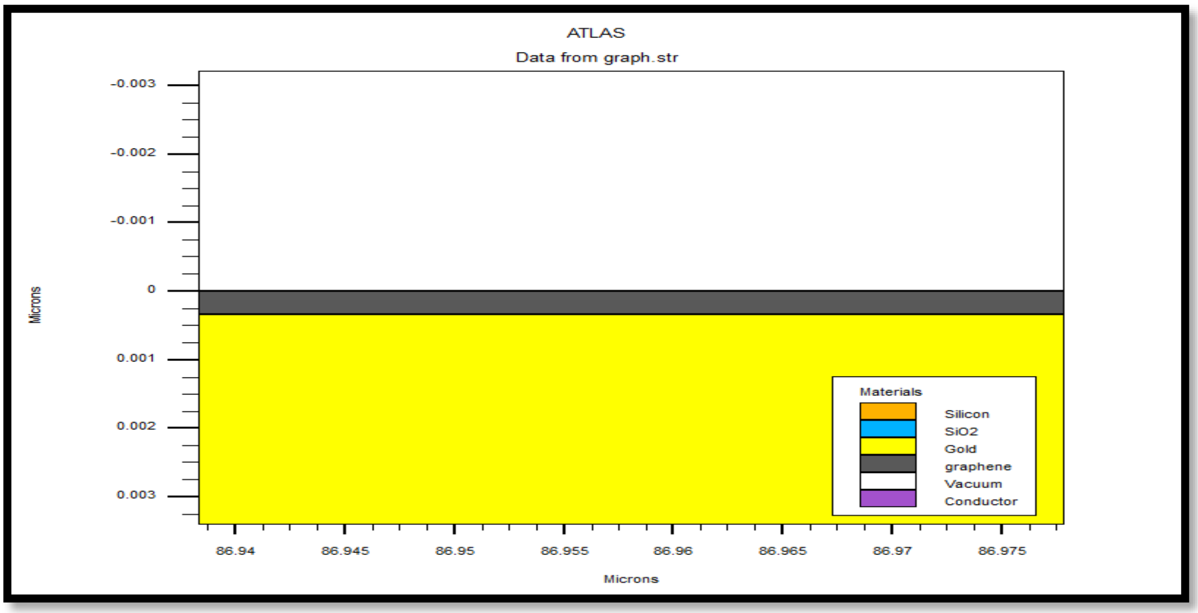

Figure 3.4: Atlas regions with materials defined.

Graphene, as a material, is not included in ATLAS material library, so to define it, we used the statement "user.material", which is used to define materials unknown to ATLAS, and we allocated it to its respective region with the position parameters.

2.2.3 Electrodes

Once the areas and materials are identified, at least one electrode that contacts the semiconductor material must be identified. This is done using the ELECTRODE statement [2].

The format to define electrodes is as follows :

ELECTRODE NAME=<electrode name><position_parameters>.

An example of created electrodes can be found in Figure 3.5

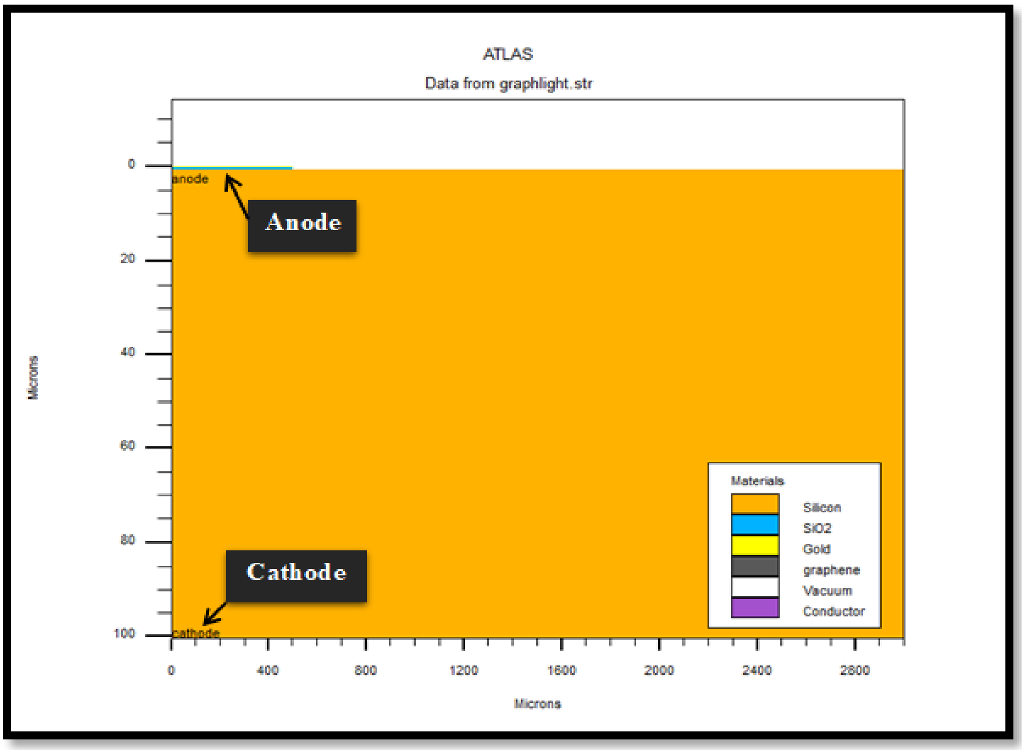

Figure 3.5: Atlas electrodes.

2.2.4 Doping

The last aspect of structure specification that needs to be defined is doping. The format of the atlas statement is as follows:

DOPING <distribution_type><dopant_type><position_parameters>.

doping uniform concentration =2e15 n-type region=1

Doping can be n type or p type.

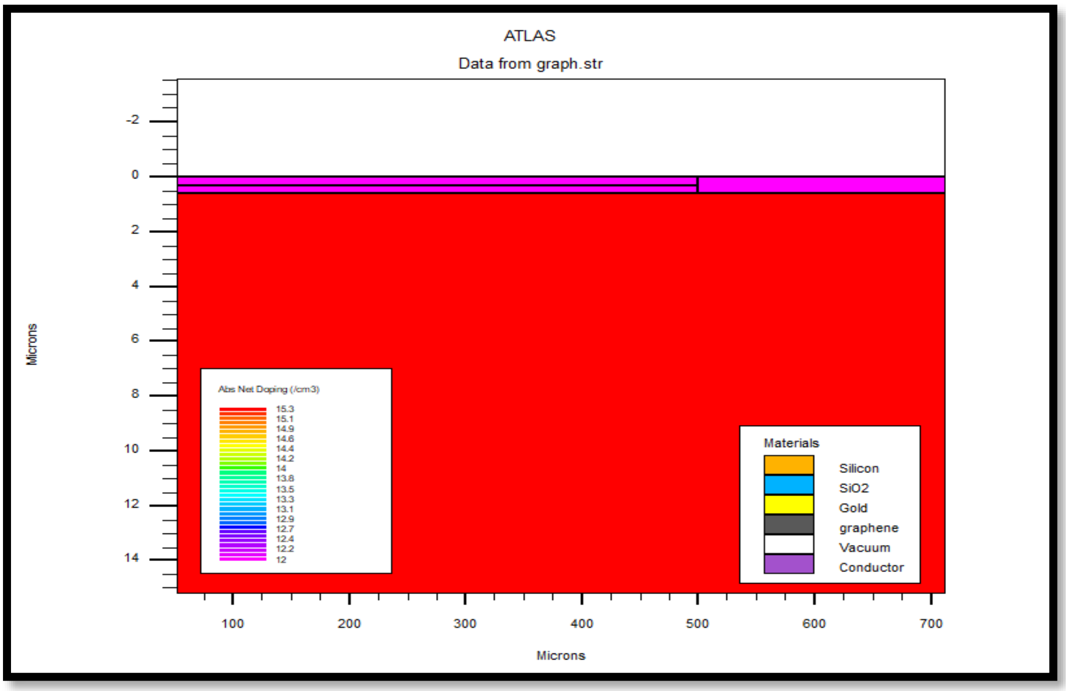

Figure3.6: The doping distribution in regions

2.3 Material Models Specification

Once the mesh, geometry, and doping profiles are defined, you can modify the characteristics of electrodes, change the default material parameters, and choose which physical models ATLAS will use during the device simulation. These actions are accomplished using the CONTACT, MATERIAL, and MODELS statements respectively.

2.3.1 Material

The format for the material statement is as follows:

MATERIAL<localization><material_definition>

A specific example used in this thesis is:

material material=graphene EG300=0.026 MUN=16983.69 MUP=16983.69 NC300=1.9e16 NV300=1.9e16 affinity=4.9 PERMITTIVITY=6 index.file=graphene.nk user.group=semiconductor user.default=4H-SIC out.index=graphene

2.3.2 Models

To get the simulation to the realistic level, a lot of complex dependencies of the device properties must be taken in consideration such as the mobility variation as a function of carriers' concentration. These complexities are not necessary in some cases, so to avoid the additional calculations,

ATALS provides independent models to describe every device property dependence alone, so they can be activated separately. The accuracy of the results obtained depends on the models used in the simulation process[61].

The physical models fall into five categories: mobility, recombination, carrier statistics, impact ionization, and tunneling. The syntax of the model statement is as follows:

MODELS <model-name>

2.4 Numerical METHOD selection

After the materials model specification, the numerical method selection must be specified. There are various numerical methods to calculate solutions to semiconductor device problems. There are three types of solution techniques used in SILVACO ATLAS:

- Decoupled (GUMMEL)
- Fully coupled (NEWTON)
- BLOCK

The GUMMEL method solves for each unknown by keeping all other unknowns constant. The process is repeated until there is a stable solution. Newton's method solves all unknowns simultaneously. The BLOCK method solves some equations with the GUMMEL method and the others with the NEWTON method.

The GUMMEL method is used for a system of equations that are poorly coupled and where there is linear convergence. Newton's method is used when equations are strongly coupled by quadratic convergence. In our example, we used the order of the following method GUMMEL NEWTON, the equations are solved by the GUMMEL method. If convergence could not be reached, the Newton method will be used to complete the calculations.

2.5 Light Beam

An optical beam is modeled as a collimated source using the BEAM statement of the form:

BEAM <parameters>

In this statement, we specified a light beam of AM1.5

2.6 Solution Specification

Solution specification can be divided up into four parts: LOG, SOLVE, LOAD, and SAVE.

• Log files (.log) store the terminal characteristics calculated by Atlas. The following shows an example of the LOG statement.

LOG OUTFILE=graphene.log.

• The SOLVE statement follows the LOG statement. SOLVE performs a solution for one or more bias points.

• The LOAD and SAVE statements are used together to help create better initial guesses for bias points. The SAVE statement saves simulation results into files for visualization or for future use as an initial guess, and after that the LOAD statement loads a solution file whenever required to assist in the solution.

2.7 Results Analysis

Once a solution has been found a semiconductor device problem, the information can be displayed graphically with TonyPlot .

Deckbuild allows extracting electrical quantities such as current short circuit (Jsc), open circuit voltage (Voc), efficiency (η) … etc. from simulation results and are stored in a file called “Results.Final” by written the statement: Extract for example:

extract name="Jsc" y.val from curve (v."anode", i."anode") where x.val=0.0

3 . Simulation results and discussions

In this part, we are going to discuss the results that we have gathered from the simulation. The variations of silicon doping, graphene thickness and work function are applied to observe their effect on the efficiency, Fill Factor, Voc and Jsc. The results are then compared with the experimental results [56].

3.1 graphene parameters used in this work

- The refractive index values of graphene depend on the optical wavelength used in simulation are represented by the following graph:

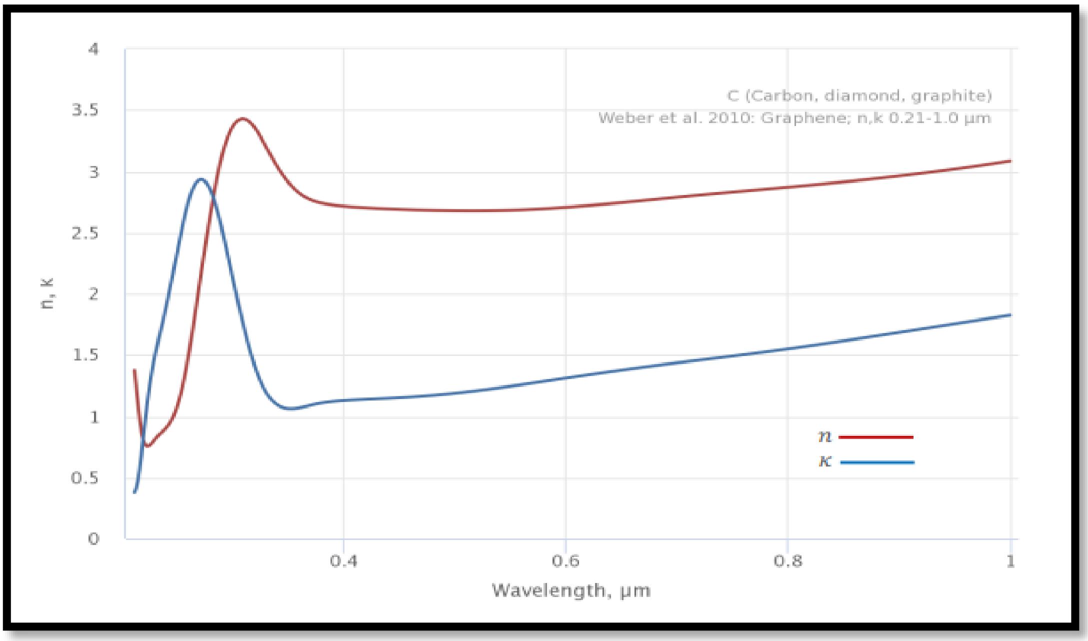

Figure3.7 : Real and Imaginary refractive index of grapheme versus optical wavelength[62].

Other important parameters of grapheme used in simulation are presented in table 3.1

Table 3.1 : The parameters of graphene that were used in the simulation

ATLAS Identifier	Value for grapheme

Bandgap (Eg)	0.026
Permittivity(ε)	6
Work function	4.8-5

3.2 Simulated structure

The simulated structure consists of 100 µm of crystalline silicon followed by a thin layer of grapheme with thickness of 10 nm deposed on all the surface except of small length on the edge dedicated for the anode which consists of two layers: the first one is a 0.3 µm of silicon oxide for the isolation between the silicon layer and the anode, the second, is another 0.3 µm of gold this time, which form the anode (see figure3.4.). The cathode is simulated as an ohmic contact in the back surface.

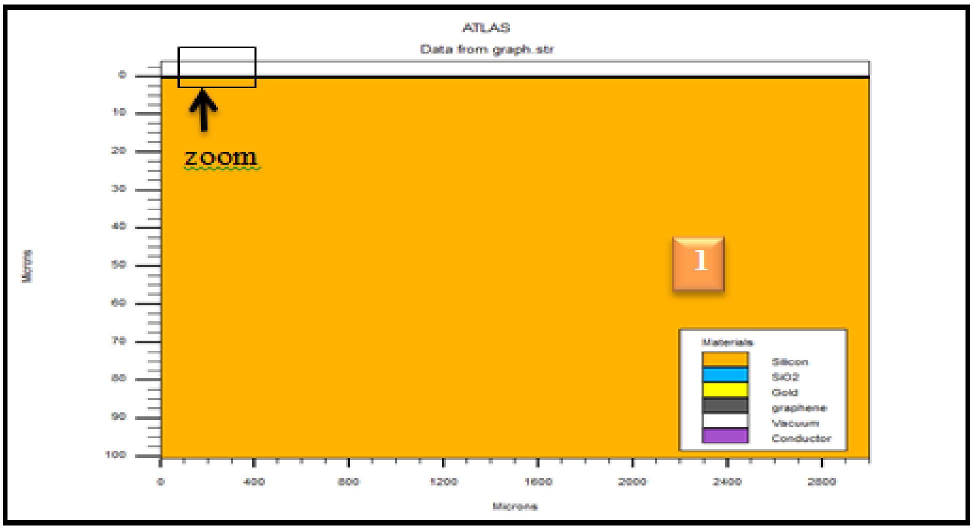

Figure 3.8.a: Atlas regions with materials defined

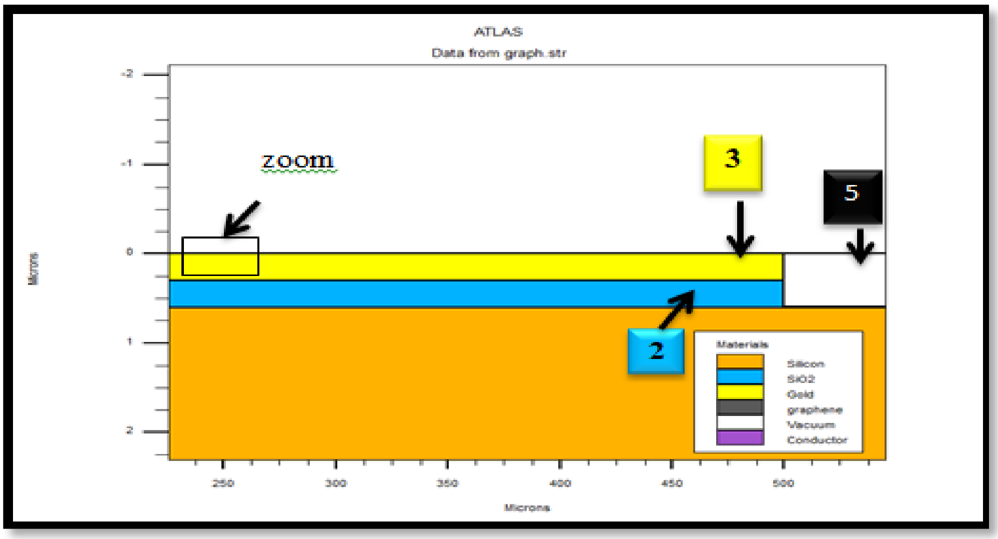

Figure 3.8.b: Atlas regions with material identification (zoom in once)

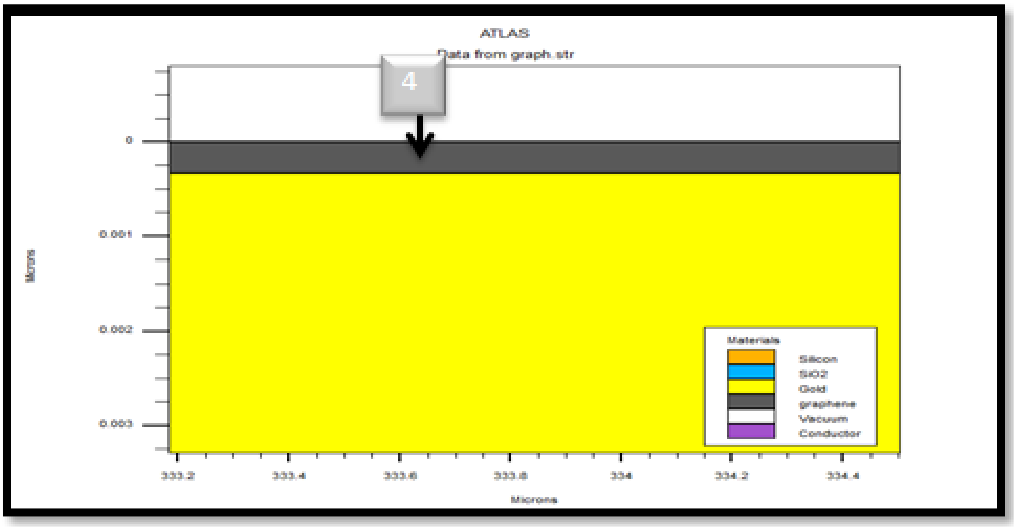

Figure 3.8.c: Atlas regions with material identification(double zoom)

- Region number (1) is Silicon
- Region number (2) is SiO2
- Region number (3) is Gold (Anode)
- Region number (4) is Graphene
- Region number (5) is Vacuum

3.3 The graphene/silicon solar cell simulation

First of all we have simulated the solar cell using the experimental parameters where the work function is between 4.8(eV) -5(eV) and silicon doping is between $1.5*10^{15}(cm^{-3})$-$3*10^{15}(cm^{-3})$ with thickness between 10(nm) and 100 (nm). in order to confirm the simulation results we have compared the experimental and the simulated results as shown in table 3.2.

Table 3.2 : Comparison Table parameters of the solar cells

Results	**Jsc ($mAcm^2$)**	**Voc (V)**	**FF(%)**	**Eff(%)**
Our results	6.81	0.42	35.66	1.02
Experimental results	4-6.5	0.42-0.48	45-56	1.65-1.34

The results show an acceptable convergence between experimental and simulation. Except for the fill factor which shows less convergence. That may be due to the fact that many parameters were not examined in the experimental parameters such as:

- The dielectric permittivity of graphene
- The optical parameters, including the refractive index that was used to obtain the optical transmittance of graphene.

3.4 Effect of graphene thickness on solar cells

We studied the effect of the graphene layer thickness on the J-V characteristic and the solar cell parameters such as open circuit voltage (Voc), fill factor (FF), short circuit current density (Jsc) and power conversion efficiency (PCE). The layer thickness is varied from 10 nm to 100 nm according to experimental reports [56] . the obtained results are shown in Figure3.9.

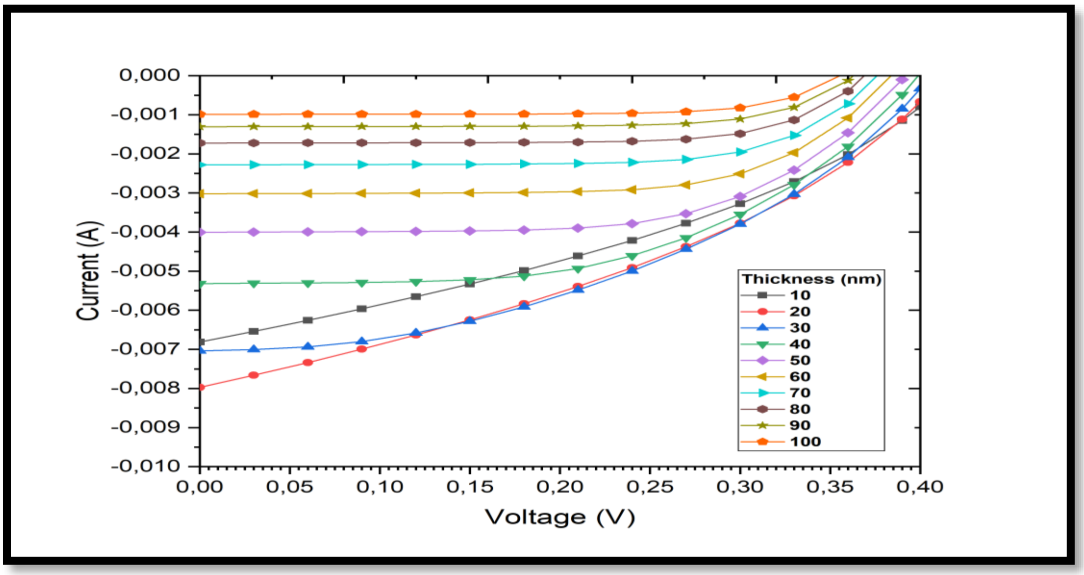

Figure 3.9 : Effect of graphene thickness on the J-V characteristic

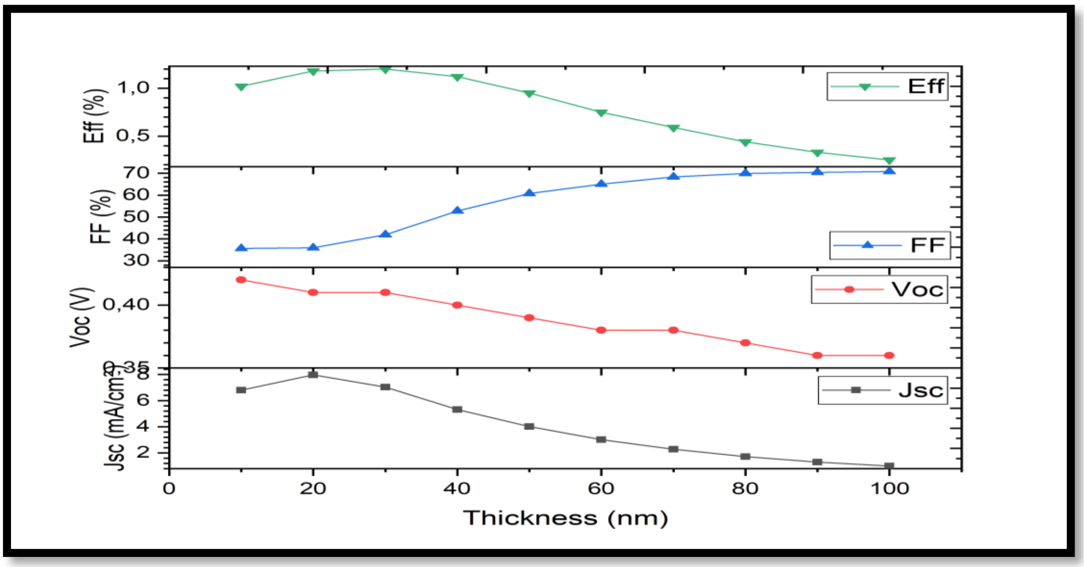

Figure 3.10: Effect of graphene thickness on the solar cell parameters

The graphs show the output parameters Jsc, Voc, FF and PCE of the solar cell versus increase in the thickness. Where we notice that there are two parts in the short circuit current density Jsc. The first part when the current density increases with increasing thickness until it reaches a maximum value of 8.17 mA/cm^{-3} corresponding to 20 nm. In the second part, the current density decreases uniformly until it reaches 0.90 mA/cm^{-3} at 100 nm. The (Voc) value is almost unchanged. The Efficiency improved from 0.9% to 1.06% and then decreased to 0.23% at 100nm.

The short circuit current Jsc increases when the series resistance decreases. The last one decreases with the increase in the contact section area, and the latter increases with the increase in the thickness and this is what happened in the first part. For the second part of the graph in which the value of Jsc is decreasing, it is related to the decrease in the photocurrent, which in turn decreases with the decrease in transmittance, which has an inverse relationship with the thickness. The decreasing series resistance has also a remarkable effect on the fill factor which is also increase with increasing thickness. On the other hand the thickness Change does not affect V_{bi} and therefore does not affect the Voc. Finally the efficiency is affected directly by the short circuit current, so it behaves like it.

3.5 Effect of doping concentration on solar cell:

In this section we will study the effect of Silicon doping on the J-V characteristic and parameters of the solar cells, open circuit voltage (Voc), fill factor (FF), the short circuit current density (Jsc) and power conversion efficiency (PCE). The Silicon doping is varied from $1*10^{15}$ (cm^{-3})- $1*10^{17}$ (cm^{-3}) as shown in figure 3.11.

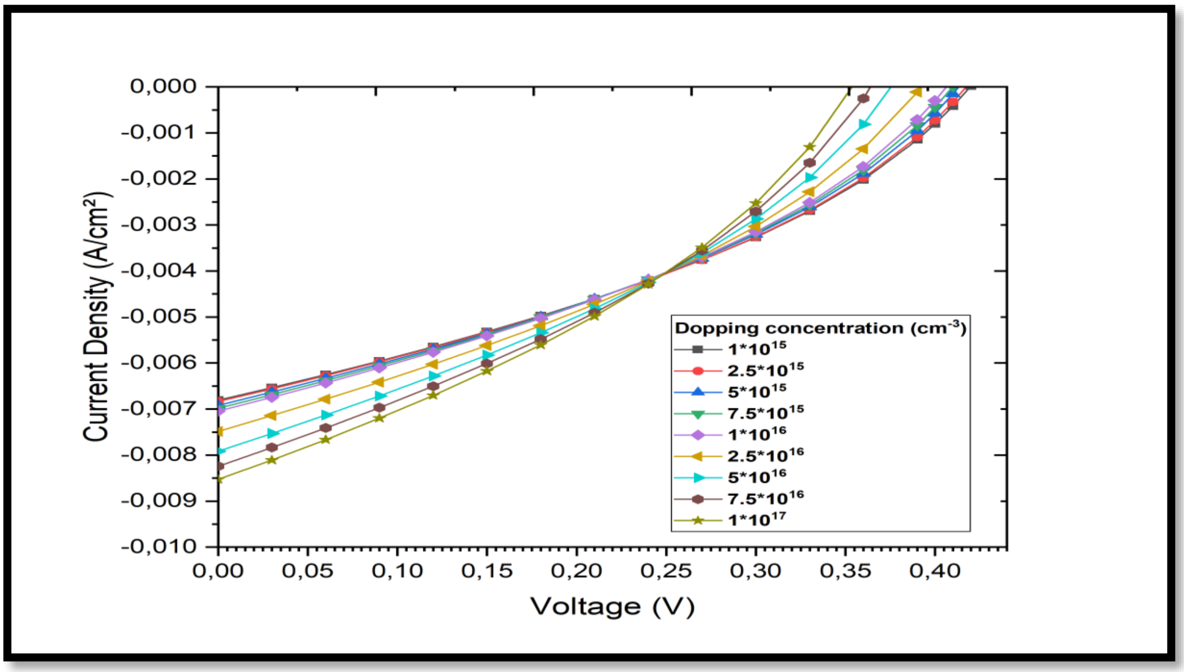

Figure 3.11: Effect of Silicon doping on the J-V characteristic

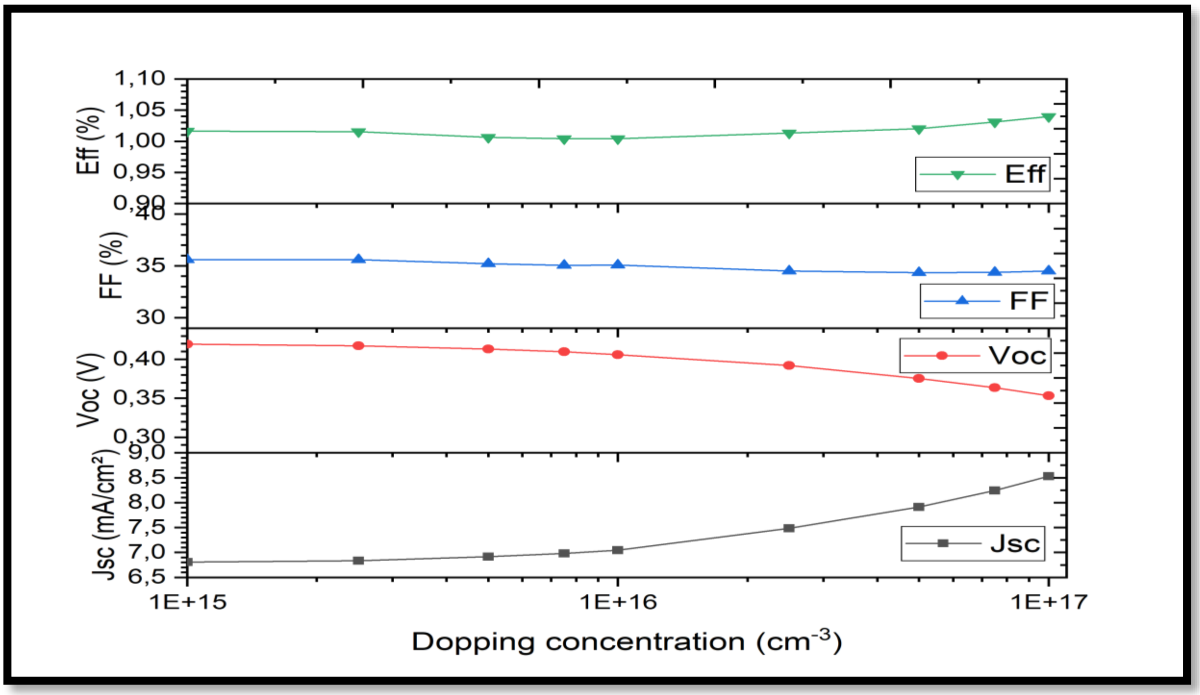

Figure 3.12: Effect of Silicon doping on the solar cell parameters

We notice that the silicon doping shows a strange effect on this solar cell. Where its increase does not affect the solar cell efficiency and has a small and neglected effect on the fill factor. On the other hand, it affects the short-circuit current and the open circuit voltage by increasing the first one from 6.80 to8.52 , and decreasing the last one from 0.41 to 0.35 . These results need more investigations; they may be affected by the schottky barrier lowering and the effect of high injection of free carriers in the thin layer of graphene.

3.6 Effect of graphene workfunction on solar cell

The effect of the work function on the parameters of the solar cells was calculated as we changed it from 4.8 (eV) to 5(eV) and summarized the results in figures (3.13 and 3.14)

The results demonstrate that with an increase in the work function of graphene, there is a significant increase in all short circuit current, open circuit voltage and efficiency where they rise from 2.25 to6.79 and from 0.23 to 0.42 from 0.27% to 1.01% respectively. While there is only a slight decrease for FF. these results can be explained as follow:

- The growth in Voc can be explained by the built in voltage. Where the work function is related directly to the built-in voltage as demonstrated in relationship (1.2).
- The increase in the short circuit current (which is also the photocurrent) can be explained by the increase the space charge region length, which is due to the growth of the work function.

- The increase in efficiency is due to the significant increase in Voc and Jsc although a slight decrease in FF which had no significant effect on Eff.

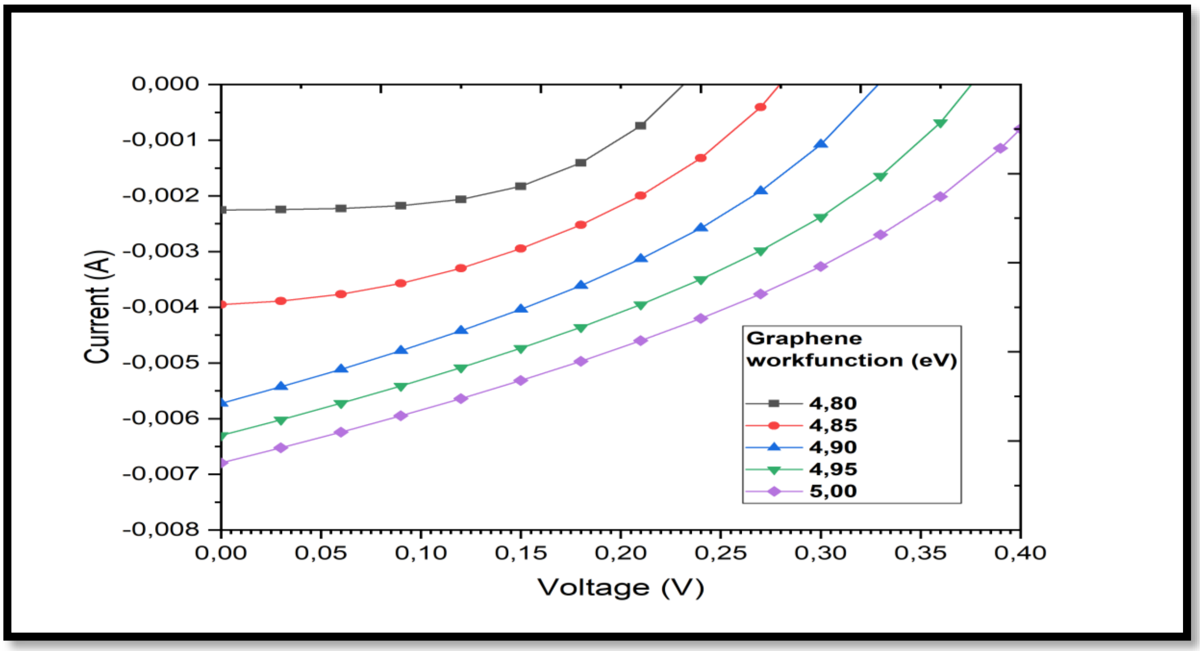

Figure 3.13: Effect of graphene workfunction on the J-V characteristic

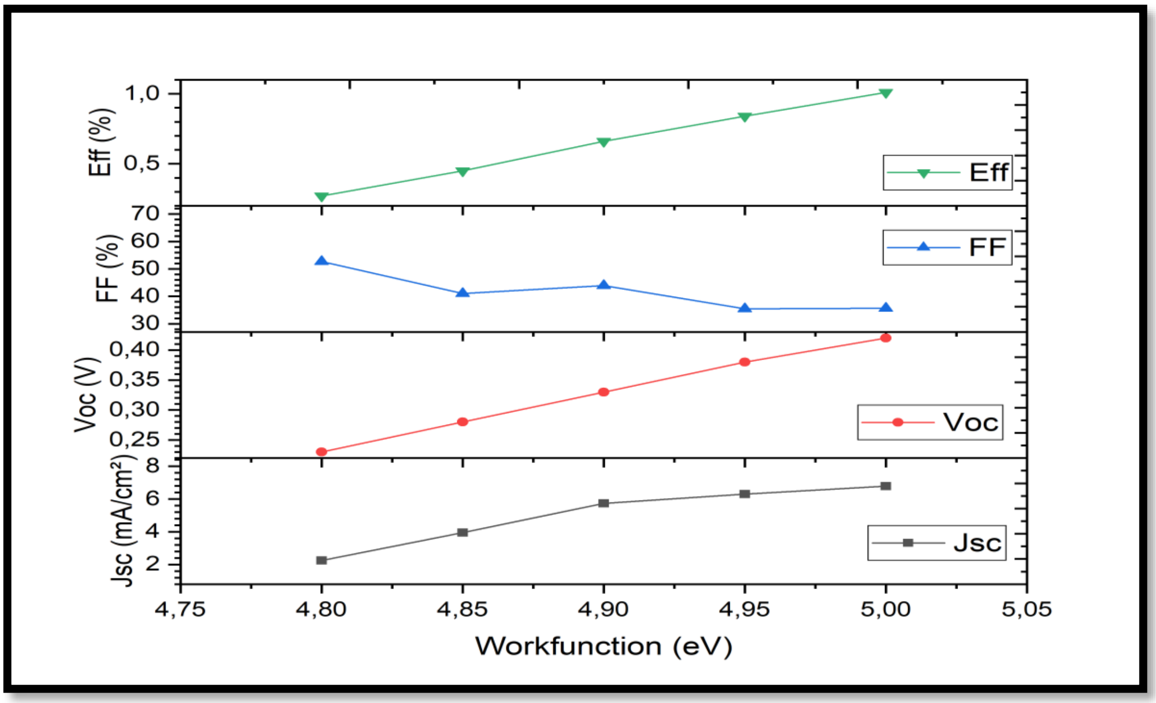

Figure 3.14: Effect of graphene work function on the solar cell parameters

Conclusion

Conclusion

In this work, we have investigated the performance of graphene-based solar cells, in order to increase the conversion efficiency, by studying some effects (such as doping, thickness, work function ...etc), by simulation using the Silvaco Atlas software.

The simulation shows an acceptable convergence between experimental and simulation results where there was a slight difference in the fill factor.

The simulation results shows also that the thickness of graphene layer can affect the solar cell efficiency by affecting the short circuit current where we have obtain a maximum value of 1.2% for 30 nm.

The second studied parameter was the silicon layer doping concentration. Which affect the Jsc and Voc differently by increasing the first one and decreasing the second. While it has no effect on the efficiency since it depends directly to Jsc and Voc. The last studied parameter which is the graphene work function has a good effect on the solar cell parameters where all of them increase by increasing the work function.

The simulation of graphene based solar cells shows a major difficulties. Therefore, other parameters and developments should be included in the simulation program in order to improve the convergence between the simulation and the experimental results. Such as the exact values of the density of states of the conduction and valence band, the solar cell shape shows also a great effect on the simulation results, therefore a 3D simulation may have better result

References

1. LASLADJ, M., *Simulation numérique des cellules solaires de troisième génération pour des applications spatiales*. 2015.
2. BAGHDADLI-née-KORTI, N., *Évolution Du paramètre exciton de BOHR EN FONCTION DES Propriétés Optoélectroniques des semiconducteurs III-V.*
3. CHABANE, H., *Etude D'une Cellule Solaire A Base De Structure Pin*. 2015, Université de Batna 2.
4. Makhèouf, M., *Etude et optimisation d'un modèle de conversion d'énergie photovoltaique. Application au pompage.* 2006.
5. Van Zeghbroeck, B., *Principles of semiconductor devices.* Colarado University, 2004. **34**.
6. Barlow, M.D., *Metal-semiconductor contacts for schottky diode fabrication*. 2007.
7. LAZNEK, S., *Simulation numérique des caractéristiques électriques d'une cellule solaire pin à puits quantiques à base de mixture d'Aluminium et d'Arséniure de Galium*. 2019, Université Mohamed Khider de Biskra.
8. Amara, K., *Contribution à l'étude de conception d'une centrale photovoltaïque de puissance (1MW) interconnectée au réseau de distribution électrique moyenne tension*. 2015, Université Mouloud Mammeri.
9. Sze, S.M. and K.K. Ng, *Physics of Semiconductor Devices*. 2006: Wiley.
10. Becquerel, M., *Mémoire sur les effets électriques produits sous l'influence des rayons solaires.* Comptes rendus hebdomadaires des séances de l'Académie des Sciences, 1839. **9**: p. 561-567.
11. Adams, W.G. and R.E. Day, *V. The action of light on selenium.* Proceedings of the Royal Society of London, 1877. **25**(171-178): p. 113-117.
12. Pauli, W., *Einstein's contribution to quantum theory*, in *Writings on Physics and Philosophy*. 1994, Springer. p. 85-94.
13. Bloch, F., *Quantum mechanics of electrons in crystal lattices.* Z. Phys, 1928. **52**: p. 555-600.
14. Wilson, A.H., *The theory of electronic semi-conductors.-ii.* Proceedings of the Royal Society of London. Series A, Containing Papers of a Mathematical and Physical Character, 1931. **134**(823): p. 277-287.
15. Carlson, D.E. and C.R. Wronski, *Amorphous silicon solar cell.* Applied Physics Letters, 1976. **28**(11): p. 671-673.
16. Fraas, L., et al. *Over 35% efficient GaAs/GaSb stacked concentrator cell assemblies for terrestrial applications*. in *Conference Record, 21st IEEE Photovoltaic Specialists Conference, Kissimimee*. 1990.
17. MOSTEFA KARA, S., *ETUDE ET SIMULATION DE CELLULES PHOTOVOLTAIQUES A COUCHES MINCES A BASE DE CIS et CIGS*.
18. Zouak, B., *Etude de l'évolution des caractéristiques des matériaux thermoélectrique des anciennes et nouvelles générations et applications photovoltaique-thermoélectricité*. 2012, Université Mouloud Mammeri.
19. Abdelkader, M., *Modélisation à deux dimensions des propriétés physiques de cellules solaires au silicium à base de substrat de type n. Étude de quelques cas particuliers de cellules innovantes*. 2017, Thèse de Doctorat En Physique. L'Université Abdel Hamid Ibn Badis de ….

20. Green, M.A., *Corrigendum to 'Solar cell efficiency tables (version 49)'[Prog. Photovolt: Res. Appl. 2017; 25: 3–13].* Progress in Photovoltaics: Research and Applications, 2017. **25**(4): p. 333-334.
21. AZZOUZI, G., *Study of silicon solar cells performances using the impurity photovoltaic effect*. 2014.
22. Standard, A., *Standard tables for reference solar spectral irradiances: direct normal and hemispherical on 37° tilted surface.* American Society for Testing Materials: West Conshocken PA, USA, 2007.
23. MALLEM, I., *Simulation des cellules solaires hétérojonction Si-SiGe par SILVACO*. 2014, Université Mohamed Khider-Biskra.
24. Honsberg, C. and S. Bowden, *Photovoltaics education website*. 2019.
25. Augusto, A., et al., *Analysis of the recombination mechanisms of a silicon solar cell with low bandgap-voltage offset.* Journal of Applied Physics, 2017. **121**(20): p. 205704.
26. Kalogirou, S.A., *Solar energy engineering: processes and systems*. 2013: Academic Press.
27. Boehm, H.P., R. Setton, and E. Stumpp, *Nomenclature and terminology of graphite intercalation compounds (IUPAC Recommendations 1994).* Pure and Applied Chemistry, 1994. **66**(9): p. 1893-1901.
28. Dybowska-Sarapuk, L., et al., *Efficient inkjet printing of graphene-based elements: Influence of dispersing agent on ink viscosity.* Nanomaterials, 2018. **8**(8): p. 602.
29. Czerniak-Reczulska, M., A. Niedzielska, and A. Jedrzejczak, *Graphene as a material for solar cells applications.* Advances in Materials Science, 2015. **15**(4): p. 67.
30. Bharech, S. and R. Kumar, *A review on the properties and applications of graphene.* J Mater Sci Mech Eng, 2015. **2**(10): p. 70.
31. Aravind, S.S.J., V. Eswaraiah, and S. Ramaprabhu, *Facile synthesis of one dimensional graphene wrapped carbon nanotube composites by chemical vapour deposition.* Journal of Materials Chemistry, 2011. **21**(39): p. 15179-15182.
32. Mijatovic, D., J.C. Eijkel, and A. Van den Berg, *Technologies for nanofluidic systems: top-down vs. bottom-up—a review.* Lab on a Chip, 2005. **5**(5): p. 492-500.
33. Mahmoudi, T., Y. Wang, and Y.-B. Hahn, *Graphene and its derivatives for solar cells application.* Nano Energy, 2018. **47**: p. 51-65.
34. Lu, X., et al., *Tailoring graphite with the goal of achieving single sheets.* Nanotechnology, 1999. **10**(3): p. 269.
35. Dalla Francesca, K., *Exfoliation du graphène par voie liquide en vue d'une application aux contacts électriques*. 2016, Université Paris-Saclay.
36. Miao, C., et al., *Chemical vapor deposition of graphene.* Physics and applications of graphene-experiments, 2011: p. 2011.
37. Salk, S.B., et al., *Croissance et caractérisation de graphène au Pôle CNFM de Lille.* J3eA, 2019. **18**: p. 1003.
38. Wang, J., et al., *High-yield synthesis of few-layer graphene flakes through electrochemical expansion of graphite in propylene carbonate electrolyte.* Journal of the American Chemical Society, 2011. **133**(23): p. 8888-8891.
39. Yu, P., et al., *Electrochemical exfoliation of graphite and production of functional graphene.* Current opinion in colloid & interface science, 2015. **20**(5-6): p. 329-338.
40. Pei, S. and H.-M. Cheng, *The reduction of graphene oxide.* Carbon, 2012. **50**(9): p. 3210-3228.

41. Cooper, D., et al., *Experimental Review of Graphene, ISRN Condensed Matter Physics, vol. 2012*. 2012.
42. Morozov, S., et al., *Giant intrinsic carrier mobilities in graphene and its bilayer.* Physical review letters, 2008. **100**(1): p. 016602.
43. Lee, C., et al., *Measurement of the elastic properties and intrinsic strength of monolayer graphene.* science, 2008. **321**(5887): p. 385-388.
44. Hancock, Y., *The 2010 Nobel Prize in physics—ground-breaking experiments on graphene.* Journal of Physics D: Applied Physics, 2011. **44**(47): p. 473001.
45. Nair, R.R., et al., *Fine structure constant defines visual transparency of graphene.* science, 2008. **320**(5881): p. 1308-1308.
46. Huang, X., et al., *Graphene-based composites.* Chemical Society Reviews, 2012. **41**(2): p. 666-686.
47. Britannica, E., *Encyclopædia britannica*. 1993, Chicago: University of Chicago.
48. Matthew, A.H. and W.J.J.o.M.S. Thomas, *What is the Young's modulus of silicon.* 2010. **19**(2): p. 229-382.
49. Methfessel, M., C. Rodriguez, and O.J.P.R.B. Andersen, *Fast full-potential calculations with a converged basis of atom-centered linear muffin-tin orbitals: Structural and dynamic properties of silicon.* 1989. **40**(3): p. 2009.
50. Zhang, Y., et al., *Graphene enabled all-weather solar cells for electricity harvest from sun and rain.* Journal of Materials Chemistry A, 2016. **4**(34): p. 13235-13241.
51. Kong, X., et al., *Graphene/Si Schottky solar cells: a review of recent advances and prospects.* RSC advances, 2019. **9**(2): p. 863-877.
52. Bi, H., et al., *Transparent conductive graphene films synthesized by ambient pressure chemical vapor deposition used as the front electrode of CdTe solar cells.* Advanced materials, 2011. **23**(28): p. 3202-3206.
53. Sim, J.-K., et al., *Implementation of graphene as hole transport electrode in flexible CIGS solar cells fabricated on Cu foil.* Solar Energy, 2018. **162**: p. 357-363.
54. You, P., et al., *Efficient semitransparent perovskite solar cells with graphene electrodes.* Advanced materials, 2015. **27**(24): p. 3632-3638.
55. Singh, E. and H.S. Nalwa, *Graphene-based dye-sensitized solar cells: a review.* Science of advanced Materials, 2015. **7**(10): p. 1863-1912.
56. Li, X., et al., *Graphene-on-silicon Schottky junction solar cells.* 2010. **22**(25): p. 2743-2748.
57. Di Bartolomeo, A.J.P.R., *Graphene Schottky diodes: An experimental review of the rectifying graphene/semiconductor heterojunction.* 2016. **606**: p. 1-58.
58. Zhong, H., et al., *Charge transport mechanisms of graphene/semiconductor Schottky barriers: A theoretical and experimental study*. 2014. **115**(1): p. 013701.
59. Schiavo, D., *Modeling Radiation Effects on a Triple Junction Solar Cell using Silvaco ATLAS*. 2012, NAVAL POSTGRADUATE SCHOOL MONTEREY CA.
60. Manual, A.U.s., *Silvaco International, Santa Clara, CA, USA*. 2012.
61. Rami, B., *Simulation de l'effet de la température et les défauts sur les caractéristiques électriques des diodes à base de GaAs (Simulation of the temperature and the deep traps effect on the electrical characteristics of GaAs diodes)*.
62. Weber, J., V. Calado, and M.J.A.P.L. Van De Sanden, *Optical constants of graphene measured by spectroscopic ellipsometry.* 2010. **97**(9): p. 091904.